Arabidopsis thaliana AMY3 is a unique redox-regulated chloroplastic -amylase

Seung, David ; Thalmann, Matthias ; Sparla, Francesca ; Abou Hachem, Maher ; Lee, Sang Kyu ; Issakidis-Bourguet, Emmanuelle ; Svensson, Birte ; Zeeman, Samuel C ; Santelia, Diana

Abstract: -Amylases are glucan hydrolases that cleave -1,4-glucosidic bonds in starch. In vascular plants, -amylases can be classified into three subfamilies. Arabidopsis has one member of each subfamily. Among them, only AtAMY3 is localized in the chloroplast. We expressed and purified AtAMY3 from Escherichia coli and carried out a biochemical characterization of the protein to find factors that regulate its activity. Recombinant AtAMY3 was active toward both insoluble starch granules and soluble substrates, with a strong preference for -limit dextrin over amylopectin. Activity was shown to be dependent on a conserved aspartic acid residue (Asp(666)), identified as the catalytic nucleophile in other plant -amylases such as the barley AMY1. AtAMY3 released small linear and branched glucans from Arabidopsis starch granules, and the proportion of branched glucans increased after the predigestion of starch with a -amylase. Optimal rates of starch digestion in vitro was achieved when both AtAMY3 and -amylase activities were present, suggesting that the two enzymes work synergistically at the granule surface. We also found that AtAMY3 has unique properties among other characterized plant -amylases, with a pH optimum of 7.5-8, appropriate for activity in the chloroplast stroma. AtAMY3 is also redox-regulated, and the inactive oxidized form of AtAMY3 could be reactivated by reduced thioredoxins. Site-directed mutagenesis combined with mass spectrometry analysis showed that a disulfide bridge between Cys(499) and Cys(587) is central to this regulation. This work provides new insights into how -amylase activity may be regulated in the chloroplast.

DOI: https://doi.org/10.1074/jbc.M113.514794

The Arabidopsis *At*AMY3 is a Unique Redox-regulated Chloroplastic α-Amylase*

David Seung[1], Matthias Thalmann[1,5], Francesca Sparla[2], Maher Abou Hachem[3], Sang Kyu Lee[1,6], Emmanuelle Issakidis-Bourguet[4], Birte Svensson[3], Samuel C. Zeeman[1] and Diana Santelia[1,5]

[1]Institute for Agricultural Sciences, ETH Zürich, Universitätstrasse 2, 8092 Zürich, Switzerland

[2]Department of Experimental Evolutionary Biology, University of Bologna, I-40126 Bologna, Italy

[3]Enzyme and Protein Chemistry, Department of Systems Biology, Technical University of Denmark, Søltofts Plads, Building 224, DK-2800 Kgs. Lyngby, Denmark

[4]Institut de Biologie des Plantes, UMR 8618 CNRS / Univ. Paris-Sud, Orsay, France

[5]Current address: Institute of Plant Biology, University of Zürich, Zollikerstrasse 107, 8008 Zürich, Switzerland

[6]Current address: Graduate School of Biotechnology & Crop Biotech Institute, Kyung Hee University, Yongin 446-701, Korea

*Running title: *AtAMY3 is a redox-regulated α-amylase*

To whom correspondence should be addressed: Diana Santelia, Institute of Plant Biology, University of Zurich, Zollikerstrasse 107, 8008 Zurich, Switzerland, Tel.: +41-(0)44-634-8286; Fax.: +41(0)-44-634-8204; E-mail: dsantelia@botinst.uzh.ch

Keywords: α-amylase, amylopectin, Arabidopsis, carbohydrate metabolism, plant biochemistry, redox regulation, starch, thioredoxin,

Background: *At*AMY3 is an α-amylase implicated in leaf starch degradation.
Results: *At*AMY3 releases small linear and branched glucans from starch under neutral-alkaline conditions, and is subject to reductive activation by thioredoxins.
Conclusion: *At*AMY3 is adapted for activity in the chloroplast and is a redox-regulated enzyme.
Significance: The unique properties of *At*AMY3 amongst α-amylases provide new insight into the regulation of starch degradation *in vivo*.

SUMMARY

α-Amylases (AMYs) are glucan-hydrolases that cleave α-1,4-glucosidic bonds in starch. In vascular plants, α-amylases can be classified into three sub-families. Arabidopsis has one member of each sub-family. Amongst them, only *At*AMY3 is localised in the chloroplast. We expressed and purified *At*AMY3 from *E. coli* and carried out a biochemical characterisation of the protein to find factors that regulate its activity. Recombinant *At*AMY3 was active towards both insoluble starch granules and soluble substrates, with a strong preference for β-limit dextrin over amylopectin. Activity was shown to be dependent on a conserved aspartic acid residue (Asp^{666}), identified as the catalytic nucleophile in other plant α-amylases such as the barley AMY1. *At*AMY3 released small linear and branched glucans from Arabidopsis starch granules, and the proportion of branched glucans increased after the pre-digestion of starch with a β-amylase. Optimal rates of starch digestion *in vitro* was achieved when both *At*AMY3 and β-amylase activities were present, suggesting that the two enzymes work synergistically at the granule surface. We also found that *At*AMY3 has unique properties amongst other characterised plant α-amylases, with a pH optimum of 7.5 - 8, appropriate for activity in the chloroplast stroma. *At*AMY3 is also redox-regulated, and the inactive oxidised form of *At*AMY3 could be reactivated by reduced thioredoxins. Site-directed mutagenesis combined with mass spectrometry analysis showed that a disulfide bridge between Cys^{499} and Cys^{587} is central to this regulation. This work provides new insights into how α-

amylase activity may be regulated in the chloroplast.

α-Amylases (AMYs, EC 3.2.1.1.) are endo-acting enzymes that specifically hydrolyse α-1,4 internal glucoside linkages in starch and related carbohydrates. α-Amylases occur widely among higher plants, animals, bacteria and fungi (1, 2). In vascular plants, α-amylases can be classified into three sub-families according to cellular localisation and gene structure (3). Members of each family were shown to be present in representative monocotyledons, dicotyledons and gymnosperms, and all share a conserved α-amylase active site at the C-terminus of the protein. Family one α-amylases are characterised by having a signal peptide that targets the protein to the secretory pathway. Cereal grain α-amylases are classified within this family and they are mainly active in the endosperm during mobilisation of starch. Family two α-amylases have no predicted targeting peptide and are therefore thought to localise to the cytoplasm. The function of the members of this family remains largely unknown. Family three α-amylases are characterised by a large N-terminal extension, typically 400-500 amino acids in length, which contains a predicted chloroplast transit peptide and tandem carbohydrate binding modules (CBMs). Members of this family have been shown to participate in leaf starch breakdown (4).

Much work on plant α-amylases has focused on enzymes from the cereals due to their pivotal role in the degradation of endosperm starch upon seed germination. Barley α-amylase 1 (*Hv*AMY1) and *Hv*AMY2 (both family one α-amylases) are among the most thoroughly described plant α-amylases and represent the only ones for which crystal structures are available (5). Although the two isozymes share 80% sequence identity, they differ in activity, stability and natural abundance. Towards starch granules, *Hv*AMY1 has higher activity than *Hv*AMY2, although the latter has a higher turnover rate on soluble substrates (5). Antisense suppression of an AMY1-type α-amylase in the rice endosperm leads to delayed germination, confirming its importance in starch mobilisation (6).

The importance of α-amylases in starch degradation in the chloroplasts and amyloplasts of living cells is not yet fully understood. Biochemical studies and analyses of protein sequences indicated that α-amylase is present inside plastids of some plant species (3, 7, 8). In rice, there are at least two type one α-amylase isoforms targeted to the leaf chloroplast via a Golgi-mediated secretory pathway. Notably, suppressed expression of one of the two isoforms (AMYI-1) resulted in increased starch accumulation in the young leaf tissue, suggesting that it may be involved in transitory starch degradation (6, 9).

In Arabidopsis, three genes encode α-amylase-like proteins (10). Of these genes, only α-amylase isozyme 3 (*At*AMY3) has a chloroplast transit peptide, and previous studies have confirmed its localisation in the chloroplast (10, 11). Compared to *Hv*AMY1 and other plant α-amylases, *At*AMY3 has a unique structure. Besides a highly conserved C-terminal catalytic domain, *At*AMY3 has two N-terminal starch-binding domains from the carbohydrate-binding module family 45 (CBM45; http//:www.cazy.org (12)) that would enable interaction with the starch granule surface (10, 11). Interestingly, α-glucan water dikinase (GWD), which phosphorylates starch, also possesses two N-terminal CBM45 domains with high sequence similarity to those of *At*AMY3 (11, 13). Despite being an active α-amylase, Arabidopsis plants lacking AMY3 degrade starch normally under standard growth conditions (4, 10). However, genetic analysis of mutant combinations has shown that there is a degree of redundancy in the pathway (14), such as when other starch-degrading enzymes are missing, *At*AMY3 is required for the degradation of starch (4, 15, 16). In mutant plants lacking the glucan phosphatase STARCH-EXCESS4 (SEX4), *At*AMY3 contributes to the degradation of starch at night and releases soluble phospho-oligosaccharides from the starch granule surface (4). Similarly, in plants lacking the two debranching enzymes, isoamylase 3 (ISA3) and limit dextrinase (LDA), *At*AMY3 is induced and is responsible for releasing small branched malto-oligosaccharides from the granule surface (16, 17). These data support the hypothesis that *At*AMY3 is part of the reaction network of starch degradation in the Arabidopsis chloroplast. To better understand the role of *At*AMY3 in starch degradation, we took an *in vitro* approach to unravel the functional regulation of *At*AMY3 and substrate specificity. We show that *At*AMY3 is stimulated by β-amylase activity *in vitro*, and suggest that both these activities can co-operate to achieve efficient starch degradation in the chloroplast. We also show that *At*AMY3 is unique amongst other previously described α-amylases in terms of its pH optimum and redox regulation through

a regulatory disulfide bridge. The significance of these findings in the context of Arabidopsis starch metabolism is discussed.

EXPERIMENTAL PROCEDURES

*Cloning, expression and purification of AtAMY3 recombinant protein*s – An *At*AMY3 cDNA clone (At1g69830, RAFL08-08-F08) was obtained from the RIKEN Bioresource Center (http://www.brc.riken.jp). The region encoding the full-length *At*AMY3 protein (lacking the predicted chloroplast transit peptide; amino acids 1-55) was amplified with *Bam*HI restriction sites using the following primers: 5'- CGCGGATCCATGAACAAAAGTCCCGTCGCCATTC-3' and 5'- CGCGGATCCTTAAGATGTTTCCCACACCTTGTA-3' and inserted into the pProEX HTb vector (Invitrogen, Basel, Switzerland) in frame with the N-terminal His-tag. Point mutations in the *AtAMY3* gene were generated with the QuikChange Site-Directed Mutagenesis Kit (Agilent Technologies, Basel, Switzerland) according to the manufacturer's instructions. The region encoding the full-length *At*BAM1 protein (lacking the predicted chloroplast transit peptide; amino acids 1-90) was amplified with *Eco*RI and *Sal*I restriction sites using the following primers 5'- CGGAATTCTATAGAGAAGGAGGGATTGG -3' and 5'- CGGTCGACCTAGTGAGTGAGAGCCACTG-3' and inserted into the pET28a+ vector (Invitrogen) in frame with the N-terminal His-tag. Recombinant proteins were expressed in *E. coli* BL21 (DE3) CodonPlus cells (Stratagene, Basel, Switzerland) and purified from the lysate using Ni^{2+}-NTA agarose affinity chromatography as described previously (18, 19). The fractions containing *At*AMY3 were pooled and stored in 50 mM Tris-HCl, pH 8, 10% (w/v) glycerol and 2 mM DTT. Protein concentration was determined using the Bradford assay reagent (Bio-rad, Cressier, Switzerland).

α-Amylase activity assays – *At*AMY3 amylolytic activity was assayed against the labelled substrate, blocked *p*-nitrophenyl maltoheptaoside (BPNP-G7; Ceralpha Method assay; Megazyme, Bray, Ireland) (20). Pre-mixed BPNP-G7 and thermostable α-glucosidase was purchased as the Amylase High pH Range (HR) reagent. Recombinant *At*AMY3 (10 µg) was dissolved in 60 µL 100 mM tricine-NaOH, pH 7.9. The assay was started by adding the amylase HR reagent (60 µL) and incubated for 1 h (unless specified otherwise) at 37°C. Reactions were stopped by adding 900 µL 1% (w/v) *tri*-sodium phosphate (pH 11). Released *para*-nitrophenol (PNP) was quantified spectrophotometrically (400 nm, extinction coefficient of 18.1 L $mmol^{-1}$ cm^{-1}). For *Hv*AMY1, the same assay was used but was conducted in 25 mM sodium acetate, pH 5.5, 5 mM $CaCl_2$, using 10 ng of protein assayed for 20 min. The reduced amount of protein and shorter incubation time compensated for the higher specific activity of *Hv*AMY1 as compared to *At*AMY3.

To assay the *At*AMY3 amylolytic activity on glucan substrates, purified recombinant protein (1 µg) was incubated at 25°C in 200 µL 50 mM HEPES-KOH pH 8, 1 mM $MgCl_2$, 5 mM DTT, with 1.5 mg amylopectin (Sigma-Aldrich, Buchs, Switzerland) or β-limit dextrin (Megazyme) pre-dissolved in water by heating. Reactions were stopped after 1 h by adding 200 µL 0.5 M NaOH. Blank digests were produced by substituting the enzyme with water. The MBTH (3-methyl-2-benzothiazolinone hydrazone) method was used to measure the reducing ends released during the digest (21). Briefly, 100 µL of the stopped reaction was mixed with 50 µL of MBTH reagent. The samples were heated at 80°C for 15 min, after which 100 µL 0.5% (w/v) $(FeNH_4(SO_4)_2).12H_2O$, 0.5% (w/v) sulfamic acid, 0.5 M HCl was added. The samples were cooled to room temperature and absorbance at 620 nm was measured. The amount of reducing ends released was determined against a standard curve consisting of 0-20 nmol glucose.

For activity measurements against starch granules, starch was purified from whole rosettes of wild-type Arabidopsis plants as described previously (18). The dried granules were pre-hydrated in water for one hour prior to the assay. An equivalent to 1.5 mg dry weight of granules was digested with the indicated amount of *At*AMY3 and/or *At*BAM1 in 100 mM tricine-NaOH, pH 7.9, 5 mM DTT at room temperature with end-over-end mixing on a spinning wheel. The reaction was terminated after the indicated timepoints by pelleting the starch granules, and the supernatant was heated at 95°C for 10 minutes. Soluble glucans released into the supernatant was quantified either using the MBTH method described above, or by quantifying glucose equivalents after acid hydrolysis as follows: The supernatant was mixed with an equal volume of 2 M HCl and heated at 95°C for 2 h. An appropriate volume of 1 M NaOH was added to neutralise the reaction (between pH 6-7). Glucose was quantified enzymatically using hexokinase and glucose-6-phosphate dehydrogenase as previously described (22).

Native PAGE and native PAGE blotting – Native affinity electrophoresis was performed on gels containing 7.5% (w/v) acrylamide, 9% (w/v) glycerol, 375 mM Tris-HCl, pH 8.8 and 0.1% (w/v) potato amylopectin or β-limit dextrin. The stacking gel contained 3.75% (w/v) acrylamide, 63 mM Tris-HCl, pH 6.8 and 0.1% (w/v) potato amylopectin or β-limit dextrin. Recombinant proteins in 50 mM Tris-HCl, pH 6.8, 3% (v/v) glycerol, 0.005% (w/v) Bromophenol blue were loaded onto the gel.

Total soluble proteins were extracted from leaves of four-week-old Arabidopsis plants by homogenising in 100 mM MOPS, pH 6.8, 1 mM EDTA, 1 mM DTT, 10% (v/v) ethylene glycol, 1 x Complete Protease Inhibitor Cocktail (Roche, Basel, Switzerland). Proteins in loading buffer (final concentration: 5% (v/v) glycerol, 0.005% (v/v) bromophenol blue; 30 μg per lane) were loaded onto the gel and separated by electrophoresis. For a better separation of crude extracts, we added to the gel 5 mM $MgCl_2$ and to the running buffer 2 mM $MgCl_2$. After electrophoresis, gels were incubated for 2 h in 100 mM Tris-HCl, pH 8, 1 mM $CaCl_2$, 1 mM $MgCl_2$, 5 mM DTT, at 25°C. Gels were stained in Lugol solution (Sigma-Aldrich, Buchs, Switzerland).

To determine activity under reducing and oxidising conditions, purified *At*AMY3 was reduced or oxidised prior to electrophoresis as follows: purified protein (2 μg) was mixed with 50 mM HEPES-KOH, pH 8, 1 mM $MgCl_2$, and either 5 mM DTT or 25 μM $CuCl_2$ for reducing and oxidising conditions, respectively. After incubation for 1 h at 25°C, reactions were mixed with native PAGE loading buffer and 1 μg of protein was loaded onto the gels. Reduced and oxidised samples were loaded on separate gels, and electrophoresis was carried out as described above. Gels containing the reduced protein were incubated in reducing incubation medium (described above). Gels containing the oxidised protein were incubated in an oxidising medium containing 100 mM Tris-HCl, pH 8, 1 mM $CaCl_2$, 1 mM $MgCl_2$, 100 μM $CuCl_2$. Gels were stained in Lugol solution.

For immunodetection of *At*AMY3, native gels were immersed in 2% SDS for 1 h, electroblotted onto PVDF (polyvinylidene difluoride) membrane, and probed with an antibody raised against *At*AMY3 (10) or the commercial penta-His antibody (Qiagen).

Analysis of AtAMY3 degradation products by HPAEC-PAD – Starch was purified from whole rosettes of wild-type Arabidopsis plants as described previously (18). Pre-hydrated starch granules (1.5 mg dry weight) were digested at 25°C with recombinant *At*AMY3 (10 μg) or *Hv*AMY1 (50 ng). At specified times, the starch was pelleted and the supernatant heated to 95°C for 15 min to inactivate the enzymes. The soluble degradation products in the supernatant were analysed by high-performance anion-exchange chromatography with pulsed amperometric detection (HPAEC-PAD). To debranch glucans, the supernatants were treated with isoamylase from *Pseudomonas sp.* (>500 U; Sigma) and pullulanase M1 from *Klebsiella planticola* (0.54 U; Megazyme) for 2 h at 37°C in 50 mM Na-acetate, pH 4.8. For the β-amylase digest of degradation products, the combined supernatants were treated with barley β-amylase (180 U; Megazyme) for 2 h at 37°C in 200 mM MES-KOH, 10 mM DTT, pH 6. Prior to HPAEC-PAD, samples were purified on sequential columns of Dowex 50W and Dowex 1 (Sigma) as described in (4). The degradation products were separated on a CarboPac PA200 (3 x 250 mm) column (Dionex) following these gradient conditions, where eluent A is 100 mM NaOH; eluent B is 150 mM NaOH, 500 mM sodium acetate: 0 to 13 min, a linear gradient from 95% A and 5% B to 60% A and 40% B; 13 to 50 min, a linear gradient to 15% A and 85% B; 50 to 70 min, step to 95% A and 5% B.

For pre-digestion of starch granules with β-amylase, an equivalent of 1.5 mg (dry weight) of pre-hydrated Arabidopsis starch granules was digested for 2 h at room temperature with recombinant *At*BAM1 (7.5 μg) in 100 mM tricine-NaOH, pH 7.9, 5 mM DTT. The starch was washed five times with 100 mM tricine-NaOH, pH 7.9, 2% (w/v) SDS, followed by five washes in water. The starch was then digested with *At*AMY3 as described above.

Determination of pH optimum – pH-dependent activity curves were generated using 50 mM Britton-Robinson buffer in the pH range 5-9. Buffer stocks (150 mM) were prepared as described (23) by mixing equal volumes of 150 mM acetic acid, 150 mM boric acid and 150 mM phosphoric acid, and was titrated to the appropriate pH using NaOH. Recombinant *At*AMY3 (10 μg) or *Hv*AMY1 (10 ng) was pre-incubated in Britton-Robinson buffer at each pH for 15 min, after which activity was determined against BPNP-G7.

Oxidation/reduction of AtAMY3 and redox titration – For redox modulation of *At*AMY3 activity, the recombinant protein in 100 mM tricine-NaOH, pH 7.9 was exposed to 5 mM

DTT or 50 µM $CuCl_2$ to fully reduce or oxidise the protein, respectively. After incubation at 25°C for 2 h, the reactions were desalted into fresh tricine buffer to remove DTT or $CuCl_2$. For reactivation with DTT, both the reduced and oxidised proteins (10 µg) were incubated for 2 h with 20 mM DTT in tricine buffer. Activity against BPNP-G7 was measured as described above. *Hv*AMY1 was treated as described for *At*AMY3, except all steps were carried out in 25 mM sodium acetate, pH 5.5. A lower amount of protein (10 ng) and a shorter incubation time (20 min) was used for the assay with BPNP-G7 to compensate the higher specific activity of *Hv*AMY1. For reactivation with thioredoxins (Trx), both the reduced and oxidised *At*AMY3 proteins (10 µg) were incubated with 0.05 mM DTT and Trx at 5 µM (Trx from *E coli* (Sigma), and the recombinant Arabidopsis Trx isoforms: *f1, m1, m2, m3, m4, x, y1, y2*) in a total reaction volume of 60 µL. After incubation for 30 min at 25°C, the enzyme was assayed with BPNP-G7.

For the redox titration, the fully oxidised *At*AMY3 protein (10 µg) was incubated in 60 µL of tricine buffer containing 20 mM total DTT with different ratios of dithiol:disulfide bridge. After incubating for 2 h at 25°C, the activity was measured by adding 60 µL amylase HR reagent. To calculate the midpoint redox potential, sigmoidal curves were fitted to the data using the graphing software Origin (version 8.5, OriginLab, Northampton, USA).

In-gel redox assay – Native PAGE was performed on recombinant *At*AMY3 or crude extracts as described above. After electrophoresis, one lane was excised from the gel and immersed in reducing incubation medium, whilst three remaining lanes were immersed in oxidising medium. After incubation at room temperature for the specified time, one lane from the oxidising medium and the lane incubated in the reducing medium were stained in Lugol solution. The remaining two lanes in the oxidising medium were rinsed in washing medium (100 mM Tris-HCl, pH 8, 1 mM $CaCl_2$, 1 mM $MgCl_2$) to remove excess oxidising agent. The lanes were split - one lane was incubated for the specified amount of time in wash medium whilst the other was incubated in reactivation medium (100 mM Tris-HCl, pH 8, 1 mM $CaCl_2$, 1 mM $MgCl_2$, 20 mM DTT). Both lanes were stained in Lugol solution.

MALDI-MS/MS analysis of reduced and oxidised AMY3 - Recombinant AMY3 was reduced/oxidised and subsequently buffer-exchanged into 100 mM tricine-NaOH, pH 7.9 as described above. The protein (10 µg; in 45 µL) was digested at 37°C overnight with LysC (100 ng/µL) and 6 µL RapiGest surfactant (Waters, Baden, Switzerland). The reaction was stopped by adding 3 µL HCl (1 M) and incubating at 37°C for a further 30 min. Insoluble material was removed by centrifugation, and the supernatant was then spotted directly on the target with the matrix (0.7 mg/mL α-Cyano-4-hydroxy-cinnamic acid in 85% acetonitrile, 0.1% triflouroacetic acid). The spotted sample was then washed on the target with 0.1% TFA and covered with matrix. The mass spectrometry analysis was conducted using an Ultraflextreme MALDI-TOF/TOF instrument (Bruker, Faellanden, Switzerland). MS/MS spectra were searched with Mascot software (Matrix Science; http://www.matrixscience.com) against the recombinant protein sequence.

Multiple sequence alignments of AtAMY3 – Amino acid sequences of *At*AMY3 protein orthologs from the following organisms were retrieved from the Phytozome database (24)*: Vitis Vinifera* (GSVIVT01020069001)*, Eucalyptus grandis* (Eucgr.G02543.1)*, Ricinus communis* (29736.m002033)*, Poplar trichocarpa* (POPTR_0010s10300.1)*, Carica papaya* (evm.model.supercontig_5.271)*, Arabidopsis lyrata* (339218)*, Brassica rapa* (Bra016262), *Manihot esculenta* (cassava4.1_001362m), *Phaseolus vulgaris* (Phvulv091010524m) and *Glycine max* (AMY3-1: Glyma02g02450.1; AMY3-2: Glyma08g40810.1). For *Hv*AMY1, the sequence of the mature protein without the signal peptide (first 24 amino acids) was retrieved from the Uniprot database (Uniprot ID: P00693). Alignment was carried out with ClustalW (25) on the web server (http://www.ebi.ac.uk/Tools/msa/clustalw2/) with the default parameters. Some sequences that aligned poorly with the other AMY3 sequences were removed – these were the *Medicago trunculata*, *Manihot esculenta* AMY3-2 and the *Malus domestica* sequences. These genes were either incomplete or had large sequence additions that disrupted alignment.

RESULTS

The catalytic mechanism of AtAMY3 is highly conserved – To study the biochemical properties of *At*AMY3 in comparison to *Hv*AMY1, the full length *At*AMY3 protein excluding the chloroplast transit peptide (amino acids 56-887), was expressed in *E. coli* and purified to near homogeneity as described in (11). The migration of the recombinant *At*AMY3

on SDS-PAGE was consistent with the calculated molecular mass of 93.5 kDa (Fig. 1A). *Hv*AMY1 was expressed in *Pichia pastoris* and purified as previously described (26) (Fig. 1A).

We assayed the purified recombinant proteins for amylolytic activity. Firstly, we tested the activity of the proteins against the artificial substrate, blocked *p*-nitrophenyl maltoheptaoside (BPNP-G7, a chromogenic substrate specific for endoamylases; (20)). *At*AMY3 cleaved the BPNP-G7 substrate at a linear rate for 150 min (Fig. 1B). As described previously, *Hv*AMY1 also displayed robust amylolytic activity towards the BPNP-G7 substrate. Thus, *At*AMY3 is a functional α-amylase *in vitro*, but is less active towards BPNP-G7 than *Hv*AMY1 (Fig. 1B and C), possibly due to a different specific activity. Within the *Hv*AMY1 catalytic domain, the aspartic acid residue Asp^{204} is essential for activity (27). Protein sequence alignment of mature *Hv*AMY1 with members of the AMY3-like family (as retrieved from the Phytozome database (24)) showed that the aspartic acid residue equivalent to Asp^{204} of *Hv*AMY1 is highly conserved in all AMY3-like sequences (supplemental File 1). Mutation of the corresponding amino acid in *At*AMY3 (Asp^{666}) to an asparagine (D666N) abolished enzyme activity (Fig. 1B), suggesting that this aspartic acid is critical for *At*AMY3 catalysis. It is likely that the catalytic mechanism between different families of plant α-amylases is conserved.

Next, we tested the ability of the recombinant *At*AMY3 and *Hv*AMY1 to degrade solubilised amylopectin and its derivative β-limit dextrin. After incubation for 1 h, both *Hv*AMY1 and *At*AMY3 were active on these substrates, as determined by the release of reducing sugars using the MBTH assay (Fig. 1D and E; (21)). The reaction times were such that the rate of hydrolysis was linear for both substrates (details not shown). *At*AMY3 activity was two-fold higher with β-limit dextrin compared to amylopectin (Fig. 1D). *Hv*AMY1 showed very similar substrate preferences (Fig. 1E). When assayed using native polyacrylamide gel electrophoresis (native PAGE) in gels containing amylopectin, recombinant *At*AMY3 migrated as four distinct activity bands with different electrophoretic mobility. All the detected activity bands could be attributed to *At*AMY3, as revealed by immunoblotting and tandem mass spectrometry (LC-MS/MS) of excised bands (data not shown). The peptide coverage yielded from this experiment suggested that the multiple bands do not arise from degradation products of *At*AMY3. It is likely that the multiple activity bands are due to molecular aggregation rather than biologically meaningful modifications or intermolecular interactions, since the native *At*AMY3 protein in Arabidopsis leaf extracts migrated as a single band (as seen in Fig 6D). As expected, *At*AMY3 D666N mutant showed complete loss of activity against both substrates (Fig. 1F).

AtAMY3 releases small linear and branched glucans from the starch granule surface in vitro –The preference of *At*AMY3 for a β-limit structure (polymers carrying short external chains) compared to amylopectin, suggests that during starch degradation *in vivo*, it may favour substrates generated by β-amylolysis. If so, *At*AMY3 would be expected to release smaller branched glucans from the surface of starch granules pre-treated with β-amylase.

To test this hypothesis, we investigated the activity of *At*AMY3 on starch granules purified from Arabidopsis leaves, and the impact of pre-treating these granules with β-amylase. The starch granules were incubated with *At*AMY3 recombinant protein, after which they were sedimented by centrifugation and the reducing sugars in the supernatant were quantified. The same was done for *Hv*AMY1. Significant starch breakdown by *At*AMY3 or *Hv*AMY1 alone was detected, showing that both enzymes can work directly on the granule surface. We pre-digested the granules with recombinant Arabidopsis β-amylase (*At*BAM1). After 15 min, *At*BAM1 did not continue to release reducing ends, suggesting that the exterior chains had been digested to a β-limit structure (data not shown). *At*AMY3 efficiently released reducing sugars from starch granules pre-digested with *At*BAM1, but the rate of hydrolysis slowed down after 15 min of incubation (data not shown).

Analysis by HPAEC-PAD revealed that the reducing sugars released from starch by *At*AMY3 or *Hv*AMY1 were predominantly composed of six, seven and eight glucose units (Fig. 2A; (28)). Quantifications of the peak areas in these chromatograms are presented in Table 1. *At*AMY3 released an increased amount of shorter glucans (with degree of polymerisation (DP) of 3-5) from the starch granule compared to *Hv*AMY1. When the starch was digested with *At*AMY3 for longer periods (*i.e.* 120 min vs 30 min), a reproducible enrichment of short chains with DP of 3-6 was observed (Fig. 2A and B). This was accompanied by a substantial decrease

in the proportion of longer products (DP 7-11) after the extended digest. This trend was not as evident for *Hv*AMY1, where we primarily observed an increase in the amount of glucan chains with DP of 6-7 over time (Fig. 2A and C). These data suggest that, in addition to the granule surface itself, longer soluble malto-oligosaccharides produced during starch degradation are effectively further degraded by *At*AMY3.

Some of the minor malto-oligosaccharides detected by HPAEC-PAD did not co-elute with linear malto-oligosaccharides standards, indicating that they were branched. This was confirmed by treatment of the digested samples with *Pseudomonas* isoamylase and *Klebsiella* pullulanase. The minor peaks disappeared and malto-oligosaccharides with a smaller average size and co-eluting with linear standards increased in abundance (Fig. 3A). Treatment of digested samples with *At*BAM1, which cannot metabolise branched malto-oligosaccharides, also confirmed that both *At*AMY3 and *Hv*AMY1 released branched glucans during starch hydrolysis. The major peaks disappeared, with a concomitant increase in maltose, while the minor peaks remained (Fig. 3A). When the starch granules were pre-digested with *At*BAM1, recombinant *At*AMY3 released a higher proportion of branched glucans with DP of 11-14 (Fig. 3B). This suggests that after β-amylase treatment, there are fewer external chains remaining for *At*AMY3, which then begins to cleave glucosidic bonds between branch points. Taken together, these data show that *At*AMY3 can act on both soluble and insoluble glucan substrates to release small linear and branched malto-oligosaccharides (16, 17).

AtAMY3 works synergistically with β-amylase towards efficient starch degradation – We hypothesised that the ability of *At*AMY3 to efficiently degrade β-limit structures may allow it to work synergistically with β-amylase during starch degradation. We tested this by degrading starch granules with *At*AMY3 and *At*BAM1 – both individually and together (Fig. 4). To quantify the total amount of soluble glucans released from the starch granule, we acid hydrolysed the glucans in the soluble fraction after the digest, and quantified the amount of glucose present. After an initial phase of rapid starch degradation (0 – 30 min), the rate of glucans released from the granule decreased for *At*AMY3 (Fig. 4). This decrease probably occurs as the enzyme reaches more crystalline areas of the granule that are difficult to degrade. A similar trend was observed for *At*BAM1, although we presume that β-amylase activity slows as a β-limit structure is approached. However, when both enzymes were added together, the amount of soluble glucans released from the starch granules was much higher than expected from the added individual activities of *At*AMY3 and *At*BAM1 alone. Furthermore, a steady release of glucans into the soluble fraction was sustained for up to 120 mins. These data suggest that efficient starch degradation is achieved when both enzymes are present.

AtAMY3 has a pH optimum suited for activity in the chloroplast – We assayed *At*AMY3 against the BPNP-G7 substrate at various pH (Fig. 5A). The pH optimum of *At*AMY3 was approximately 7.5. However, a broad peak in catalytic activity (>90% of the maximum) was observed between pH 7 and 8.5. A similar pH-activity curve was obtained when amylopectin was used as a substrate (data not shown). In contrast, *Hv*AMY1 showed a pH optimum at around 5.5, and retained only 13% of its maximum activity at pH 8 (Fig. 5B; (27)). The differences in optimal pH between the chloroplastic *At*AMY3 and the secreted barley AMY1 matched their respective subcellular localisations. The physiological pH range in the chloroplast ranges from neutral (pH 7) at night to slightly alkaline (pH 8) during the day (29). Thus, *At*AMY3 would be highly active at all stromal pH conditions. *At*AMY3 represents a rare example of plant α-amylase that is more active under alkaline than acidic conditions.

AtAMY3 activity is redox regulated – Several enzymes involved in starch metabolism have been shown to be sensitive to changes in redox potentials *in vitro* (30–35). Recently, *At*AMY3 was reported to be dependent on the reducing agent dithiothreitol (DTT) for activity against amylopectin, suggesting that it could be redox regulated (35). We investigated this hypothesis further. We found that *At*AMY3 could be inactivated by exposing the enzyme to increasing concentrations of the oxidants copper chloride ($CuCl_2$) or hydrogen peroxide (H_2O_2). Amylolytic activity against the BPNP-G7 substrate was efficiently suppressed after a 1 h treatment with 25 to 50 μM $CuCl_2$, or 2 to 4 mM H_2O_2 (data not shown). We then investigated whether the loss of activity under oxidising conditions was reversible. Fully-reduced or fully-oxidised *At*AMY3 was desalted to eliminate excess DTT or $CuCl_2$, and then incubated for 2 h with or without 20 mM DTT (Fig. 6A). Incubation with DTT had no effect on the

activity of the reduced enzyme, which showed a consistent specific activity of 28 ± 1 nmols PNP released min^{-1} mg^{-1}. In contrast, upon reduction of fully-oxidised inactive *At*AMY3 with an excess of DTT, activity was restored to about 65% of the original activity (Fig. 6A). This indicates that *At*AMY3 could be reversibly inactivated and activated depending on its redox state, even though a fraction of the protein seems to have been irreversibly oxidised. For comparison, we exposed *Hv*AMY1 to the same treatment. In contrast to *At*AMY3, *Hv*AMY1 lost only 14% of its fully reduced activity after treatment with 50 μM $CuCl_2$ for 2 h (Fig. 6B). Given that $CuCl_2$ is a thiol oxidising agent, we concluded that *Hv*AMY1 was virtually redox-insensitive. To our knowledge, no other α-amylase has been previously reported to be redox regulated. Thus, redox-sensitivity is not a common feature of plant α-amylases, but rather one specific to *At*AMY3. The redox-regulation of *At*AMY3 can be seen as another adaption for activity in the chloroplast.

To test whether changes in the redox conditions affected *At*AMY3 activity towards amylopectin, we developed an in-gel redox assay using native gels (See experimental procedures for details). After electrophoresis of purified *At*AMY3, individual lanes were treated with 5 mM DTT or 25 μM $CuCl_2$ for 1 h prior to staining with iodine solution. *At*AMY3 activity was detected only in lanes that had a reducing treatment, consistent with the BPNP-G7 assay results (Fig. 6C). Lanes treated with $CuCl_2$ were rinsed to remove excess oxidising agent, and then re-incubated with or without 20 mM DTT for 3 h before staining with iodine. DTT treatment restored the amylolytic activity of the protein. Hence, the activity of recombinant *At*AMY3 towards amylopectin is modulated by changes in redox potential. A redox-sensitive amylolytic activity corresponding to *At*AMY3 was also observed when Arabidopsis leaf crude extracts were analysed using amylopectin-containing native gels exposed to the same treatment as described above (Fig. 6D), suggesting that native *At*AMY3 from leaf extracts is similarly redox regulated.

To investigate whether *At*AMY3 activity responds to physiologically meaningful redox potentials, we conducted a redox titration analysis in which defined mixtures of $DTT_{reduced}$ and $DTT_{oxidised}$ were used as a redox equilibration buffer. Enzyme activity against BPNP-G7 was assayed after the oxidised *At*AMY3 was allowed to equilibrate for 2 h at the different redox potentials. At pH 7.9, *At*AMY3 shifted from an active form at – 400 mV to an inactive form at – 280 mV, confirming that the protein was mostly active under reducing conditions (Fig. 7). We estimated the midpoint redox potential (E_m) by fitting the Nernst equation to the data, and obtained a value for *At*AMY3 of -329 ± 2 mV. This is within the range reported for other redox regulated chloroplast enzymes, including the β-amylase BAM1 (-350 mV at pH 7.9; (32)), and the glucan, water dikinase GWD (-310 mV at pH 7.9, (31)). Hence, the redox sensitivity of *At*AMY3 appeared to be within a physiologically meaningful range.

Chloroplastic thioredoxins can reactivate the oxidised AtAMY3 in vitro – In plants, thioredoxins (Trxs) directly reduce their target redox-regulated enzymes by performing disulfide exchange reactions (36). We determined the ability of *At*AMY3 to interact with Trxs *in vitro*. The isoforms tested included a commercially available recombinant Trx from *E. coli*, as well as chloroplastic Trxs from Arabidopsis, which were obtained as recombinant proteins (37, 38). Co-incubation of 5 μM Trx with 0.05 mM DTT in the reactivation treatment resulted in a drastic stimulation of *At*AMY3 activity compared with DTT treatment alone (Table 2). The activity reached a maximum after 30 min of reduction (details not shown). These data revealed that *At*AMY3 is efficiently reduced by Trxs. The chloroplast Trxs, however, showed selectivity in their interaction with *At*AMY3. Trx *f1* proved most effective, displaying a similar reactivation efficiency (59%) to that observed using 20 mM DTT for 2 h (65%, Fig. 6A). This is consistent with previous observations that the majority of Trx-regulated enzymes in starch metabolism are most efficiently activated by Trx *f*. Given that Trx can only reduce its target protein through a thiol/disulfide exchange mechanism (36), our results implicate the reduction of a disulfide bridge between different cysteine residues in the process of *At*AMY3 activation.

Mechanism of AtAMY3 redox-dependent reactivation – Nine cysteine residues are present in the amino acid sequence of *At*AMY3. Of these residues, four (C118, C285, C310 and C363) are located in the N-terminal extension, and five (C499, C587, C652, C743 and C832) in the α-amylase domain (supplemental File 1). We performed site-directed mutagenesis on these cysteines to investigate the importance of each residue for disulfide formation in *At*AMY3. Each mutated *At*AMY3 variant, carrying a single

cysteine to serine substitution, was produced in *E. coli* and purified as a soluble product.

*At*AMY3 Cys-mutants were all active under reducing conditions, but the level of activity varied. *At*AMY3 C587S showed lower activity against both BPNP-G7 and amylopectin compared to the wild-type *At*AMY3 (Fig. 8A and Table 3). *At*AMY3 C285S and C652S also had slightly reduced activity, whereas C499S was virtually inactive. In contrast, the C363S mutant displayed higher activity. It is possible that these mutations change the stability or conformation of the proteins, altering their catalytic activity. Notably, under oxidising conditions, C587S was the only *At*AMY3 Cys-mutant to retain amylolytic activity (Fig. 8B and Table 3). All other site-directed mutants were inactivated under oxidising conditions, and all of them could be re-activated under reducing conditions (Fig. 8C and D). These findings indicate that Cys^{587}, in addition to being important for optimal catalytic rate, is also involved in the redox-regulation of *At*AMY3 activity.

Structural mechanism for the redox-regulation of AtAMY3 - Site directed mutagenesis revealed Cys^{587} as an essential residue for the redox regulation of *At*AMY3. However, two cysteines are required to form an inhibitory disulfide bridge. We explored the possibility that *At*AMY3 may form intermolecular disulfide linkages via Cys^{587} residues using non-reducing PAGE. However, no high molecular weight bands corresponding to joined *At*AMY3 proteins were detected under oxidising conditions (data not shown). Since this finding rather suggested an intramolecular disulfide linkage, we used mass spectrometry to compare peptides generated after a proteolytic digest of reduced and oxidised *At*AMY3. Following digest with the protease, LysC, peptides were analysed by MALDI-MS/MS and resulting spectra were searched against the recombinant protein sequence with Mascot software. The sequence coverage obtained was 53.2% and 43.5% respectively for reduced and oxidised proteins. A peptide containing Cys^{587} was identified at 1679.9 m/z and confirmed by MS/MS with a high Mascot score (Fig. 9A, Table 4). We found that the abundance of this peptide was dramatically reduced in the digested oxidised protein in comparison to the reduced protein (Fig. 9A). This is consistent with the hypothesis that Cys^{587} is involved in a redox-dependent modification. We also found that the abundance of a Cys^{499} containing peptide at 2361.1 m/z showed a similar change depending on redox state (Fig. 9B, Table 4). These data suggest that a disulfide bridge may form between Cys^{499} and Cys^{587}.

We then investigated whether a joined peptide linked by Cys^{499} and Cys^{587} could be detected after digesting the oxidised protein. We identified a peptide at 4038 m/z, corresponding to the additive mass of the Cys^{587} and Cys^{499} containing peptides. This peptide was only found after digesting the oxidised wild type protein, and not the reduced protein (Fig. 9C). Additionally, the peptide was also not detected after digesting the oxidised C499S and C587S site-directed mutants, confirming that both cysteines are involved in forming this mass. Furthermore, the peptide produced a typical fragmentation pattern for disulfide-linked peptides in the MS/MS spectrum (data not shown). These data suggest that the structural basis of *At*AMY3 redox regulation is a disulfide bridge formed between Cys^{499} and Cys^{587} that inhibits catalysis. It should be noted that aside from this regulatory role, both cysteines are likely to play an important role in the activity of the enzyme, possibly by contributing to structural stability. The activity towards both amylopectin and BPNP-G7 is reduced or almost undetectable for C587S and C499S mutants respectively.

DISCUSSION

Despite conserved catalytic mechanism, AtAMY3 is adapted for chloroplastic activity – In this study, we have characterised some biochemical aspects of chloroplastic α-amylase 3 from *Arabidopsis thaliana* (*At*AMY3). Our results show that the purified heterologous *At*AMY3 protein was active against the artificial substrate BPNP-G7, against soluble substrates such as amylopectin (Fig. 1B, D, F), and against the starch granule surface (Fig. 2-4). Site directed mutagenesis of the aspartic acid residue Asp^{666} in *At*AMY3 led to complete loss of activity towards all tested substrates (Fig. 1B and F). This aspartic acid is located within the active site of other α-amylases like *Hv*AMY1 (27) and is highly conserved among members of the entire α-amylase superfamily, including debranching enzymes and glucosidases from bacteria and animals (2, 39). Thus, Asp^{666} likely represents the catalytic nucleophile of *At*AMY3. Interestingly, *Hv*AMY1 was three orders of magnitude more active than *At*AMY3 (Fig. 1B and C), the molecular basis of which is unclear. This difference in kinetics may reflect the differences in starch metabolism between the

tissues in which each enzyme is active. Cereal α-amylases are involved in rapid endosperm starch hydrolysis, and higher activities lead to better germination vigour (40). The involvement of β-amylase in this process is unclear (41). In contrast, the degradation of starch in leaf mesophyll cells is a highly regulated process. Leaf starch is degraded at a rate such that reserves accumulated during the day are sufficient for the whole night. Premature exhaustion of starch would lead to starvation at night and inhibition of growth (42, 43). It is possible that the slower kinetics of *At*AMY3 is an inevitable consequence of the regulatory features described here necessary to control the degradation of transitory starch in leaves. Furthermore, despite the slower kinetics, we demonstrated that *At*AMY3 is capable of efficient starch degradation together with β-amylase activity (Fig. 4), which is essential for leaf starch degradation (44).

β-limit dextrin at the starch granule surface is a substrate of AtAMY3 in vitro – During starch breakdown in leaf chloroplasts, reversible glucan phosphorylation allows continuous degradation by β-amylases until they reach the branch points at the root of each amylopectin cluster. Recent circumstantial evidence from *in vivo* studies suggests that the resulting β-limit dextrin structure at the granule surface is a suitable substrate for *At*AMY3. Although *At*AMY3 cannot hydrolyse α-1,6-linkages, it can access chains beyond the branch points, thereby releasing branched malto-oligosaccharides into the chloroplast stroma for subsequent metabolism by the debranching enzymes ISA3 and LDA. In *isa3lda* mutants, soluble branched glucans accumulate during the night, but are absent in the *amy3isa3lda* triple mutant (16, 17).

In accordance with this model, when tested against amylopectin and β-limit dextrin, *At*AMY3 had a strong preference for β-limit dextrin (Fig. 1D and F). A likely explanation for this is that the shorter external chains provide less steric hindrance to endoamylolytic cleavage sites. When tested against purified Arabidopsis starch granules, linear glucans with DP 6-8 are the predominant degradation products (Fig. 2A). However, when starch granules were pre-treated with *At*BAM1 (to generate a β-limit dextrin structure at the granule surface), *At*AMY3 released a higher proportion of small branched glucans from the starch granule surface (Fig. 3B). Intriguingly, after an initial period of rapid activity, the release of reducing sugars by *At*AMY3 from β-amylase pre-treated granules decreased (data not shown). In contrast, the release of reducing sugars by *At*AMY3 was sustained for longer when acting against granules that had not been pre-treated. The reason for this is unclear. It is possible that the activity of *At*AMY3 slows when faced with more crystalline regions inside the granules (as observed in Fig. 4) and that such regions are reached more rapidly by *At*AMY3 after the pre-treatment of the granules by *At*BAM1. However, efficient starch degradation was sustained for extended periods when both *At*AMY3 and *At*BAM1 was present in the digest (Fig. 4). We suggest that *At*AMY3 stimulates β-amylolytic activity at the granule surface by cleaving past branch points and releasing small, branched glucans for further degradation by debranching enzymes or *At*AMY3 itself (Fig. 2-3). Meanwhile, β-amylolytic activity stimulates *At*AMY3 by generating β-limit structures at the granule surface, which *At*AMY3 can degrade. This observed synergistic effect between the enzymes provides insight into the role of *At*AMY3 in the reaction network of starch degradation in the Arabidopsis chloroplast.

The regulatory role of Cys^{499} and Cys^{587} in AtAMY3 redox-dependent activity – In this work, we showed that *At*AMY3 has the characteristics of a redox-regulated enzyme. Both the recombinant protein and the native protein in crude extracts had a similar redox sensitivity (Fig. 6C-D), suggesting that the endogenous enzyme has a similar chemistry *in vivo*. We observed that the shift between the active, reduced form and the inactive, oxidised form occurs at physiologically relevant redox potentials. The ability of the chloroplast thioredoxins to reactivate *At*AMY3 strongly suggests that the redox regulation occurs at physiologically relevant redox potentials via a disulfide exchange (Fig. 7, Table 2). Our data also provides evidence that an intramolecular disulfide bridge between residues Cys^{499} and Cys^{587} exclusively forms under oxidising conditions. It is likely that the formation of this disulfide bridge leads to the inactivation of the enzyme, possibly by altering the tertiary structure of the protein in a way that blocks the active site. This type of mechanism was documented in the Calvin cycle enzyme, phosphoribulokinase (45). Also, in the phosphoglucan phosphatase SEX4, the catalytic Cys^{198} is involved in disulfide formation (34). A similar mechanism is likely for *At*AMY3 due to

the close proximity of Cys^{587} to the active site, which can be inferred from two lines of evidence. Firstly, Cys^{587} is highly conserved amongst α-amylases (supplemental File 1), and the corresponding cysteine residue in *Hv*AMY1 has been previously shown to be important for catalysis (46). Secondly, Cys^{587} is located two residues away from His^{585} of *At*AMY3, which aligns with His^{117} of *Hv*AMY1 (or His^{93} of mature protein) and functions as a transition state stabiliser. Substitution of His^{93} by Asn (H93N) leads to a sharp decrease in activity (27). The close proximity of Cys^{587} to the active site may also explain why the C587S mutant was less active than the wild-type protein (Fig. 8 and Table 3). Meanwhile, the site-directed mutant, C499S, was almost completely inactive against all substrates tested. It is possible that the Cys^{499} residue, like Cys^{587}, also has a role in catalysis. Since Cys^{587} is located close to the active site, it is likely that Cys^{499} is located nearby, since disulfide bridges occur between two proximal cysteines. Other site-directed mutants with low activities included C285S and C652S, suggesting they may also contribute to the activity or stability of the protein.

Interestingly, Cys^{499} is generally conserved in most but not all AMY3 sequences examined. All examined sequences from species belonging to the order Malpighiales (*Ricinus communis*, *Manihot esculenta* and *Poplar trichocarpa*) instead had a leucine residue at this position (supplemental File 1). It should be noted that there are differences in how starch is metabolised between different species, and some plants do not store and degrade starch diurnally as in Arabidopsis (47). Therefore, it is possible that a loss of AMY3 redox-regulation in the abovementioned species may reflect altered regulatory requirements in their starch metabolism. Alternatively, although Cys^{499} was the only Cys residue that formed disulfide bridges with Cys^{587} in our experiments with *At*AMY3, AMY3 in these Malpighiales species may be redox-regulated via a disulfide bridge between Cys^{587} and a different partner cysteine residue. All species that have a leucine residue instead of Cys^{499} also have an additional cysteine residue 11 amino acids upstream. This cysteine is not present in most AMY3 sequences, including *At*AMY3. Due to its close proximity to Cys^{499} on the primary structure, we speculate that this may be an alternative partner cysteine for a disulfide bridge.

Redox-regulation via disulfide exchange allows the reversible inactivation of the enzyme, and the inactive oxidised *At*AMY3 was substantially reactivated by reduction. The loss of the 35% of *At*AMY3 amylolytic activity during reactivation is most likely due to the irreversible oxidation of either regulatory cysteine to the sulfinic acid form (Cys-SO_2H) which cannot be reduced by Trx or DTT included in the assay mixture. The fact that *At*AMY3 is redox regulated contrasted markedly with *Hv*AMY1, which we found to be redox insensitive under the same conditions (Fig. 6B). However, there is some evidence that α-amylases in the endosperm of cereal grains could be indirectly influenced by redox status (48). Therefore, redox-dependent α-amylase activity in germinating grains cannot be ruled out and further investigations will be necessary to answer this question.

Significance of a redox-regulated α-amylase in transitory starch degradation – In chloroplasts, the paradigm for redox regulation of target enzymes is that regulation is light dependent, mediated by thioredoxins using electrons derived from photosystem I during photosynthesis (49). Light-activated Trxs directly reduce their target enzymes, thereby linking the availability of light to the activity of numerous enzymes (50). According to this view, redox sensitive enzymes in chloroplasts are mainly active during the day and inhibited during the night. The light-dependent redox activation of enzymes of the Calvin cycle and starch biosynthesis by reduced Trx is intuitively relevant, as it ensures coordination between photosynthesis and accumulation of starch in response to light (51). Conversely, redox regulation of enzymes involved in starch degradation, such as GWD, SEX4 and BAM1 (31, 32, 34), is counter-intuitive, as it would imply that these enzymes would be more active during period of starch synthesis and not degradation.

In the case of *At*AMY3, the broad pH optimum and the Trx-mediated redox regulation suggest that *At*AMY3 activity may be promoted during the day. However, with the available evidence, it is difficult to imagine *At*AMY3 playing a role in starch synthesis during the day. The *amy3* mutant synthesises the same amount of starch as wild-type plants (10), and knockouts of *amy3* in combination with other enzymes involved in starch degradation result in more starch accumulation rather than less (4, 15, 16). Also, in rice, the antisense suppression of the chloroplastic AMYI-1 isoform leads to more

starch in leaves (6) suggesting that chloroplastic α-amylases participate in starch breakdown.

These observations lead to speculation about the biological meaning of redox regulation of enzymes involved in the starch degradation pathway. Firstly, redox-regulation is not necessarily a diurnal on/off switch, and pH and redox potentials are not independent of each other. The midpoint potential for GWD was -310 mV at pH 7.9, but was calculated to shift to about -255 mV at pH 7.0, assuming the slope of E_m vs. pH to be 59 mV/pH unit (31). Since -255 mV is the most positive known E_m value of any enzyme involved in starch degradation, the protein may not be fully oxidised during the night. Similarly, the midpoint redox potential of *At*AMY3 would shift from -329 mV at pH 7.9 (Fig. 5) to -276 mV at pH 7. A previous study found that at pH 7 and -276 mV, Trx *f* is not completely oxidised (52). Thus, even during the night, *At*AMY3 might also not be completely oxidised and its redox regulation may be considered as a fine-tuning of activity. Secondly, a light-independent plastidial NADP-thioredoxin reductase (NTRC) could be involved in the redox regulation of starch degrading enzymes at night. Unlike Trxs, NTRC uses NADPH produced via the oxidative pentose phosphate pathway as a source of reducing power (53). BAM1 was shown to be reactivated by NTRC *in vitro*, although it appears that NTRC is not as effective as Trx *f* at reactivating the enzyme (54). Thus, it will be interesting to test whether NTRC can also reactivate *At*AMY3 *in vitro*. Finally, the presence of a redox-regulated, stress-induced starch degradation pathway has been proposed as an explanation for the Trx induced activation of BAM1 (54). Although BAM1 has a marginal role in starch degradation in mesophyll chloroplasts (44), BAM1 expression and activity are induced by osmotic stress and *bam1* mutants fail to degrade starch in response to this stress (54). BAM1 may then induce starch degradation in the light to produce maltose as an active response against the osmotic stress (54, 55). Starch degradation in the light involving β-amylase activity has also been demonstrated under photorespiratory conditions in Arabidopsis (56). Similarly to *bam1*, the *amy3* mutant also has a wild-type phenotype under standard growth conditions (10). However, *At*AMY3 expression is increased after cold shock, and *amy3* mutants accumulate more starch and less soluble sugars than in wild-type plants in response to this stress (57). Thus, redox regulation of *At*AMY3 activity may become significant during stress responses.

REFERENCES

1. Søgaard, M., Abe, J., Martin-Eauclaire, M. F., and Svensson, B. (1993) α-Amylases: structure and function. *Carbohydrate Polymers* **21**, 137–146

2. MacGregor, E., Janecek, S., and Svensson, B. (2001) Relationship of sequence and structure to specificity in the α-amylase family of enzymes. *Biochimica et Biophysica Acta* **1546**, 1–20

3. Stanley, D., Fitzgerald, A., Farnden, K., and MacRae, E. (2002) Characterisation of putative α-amylases from apple (*Malus domestica*) and *Arabidopsis thaliana*. *Biologia* **57**, 137–148

4. Kötting, O., Santelia, D., Edner, C., Eicke, S., Marthaler, T., Gentry, M. S., Comparot-Moss, S., Chen, J., Smith, A. M., Steup, M., Ritte, G., and Zeeman, S. C. (2009) STARCH-EXCESS4 is a laforin-like phosphoglucan phosphatase required for starch degradation in *Arabidopsis thaliana*. *Plant Cell* **21**, 334–346

5. Robert, X., Haser, R., Gottschalk, T. E., Ratajczak, F., Driguez, H., Svensson, B., and Aghajari, N. (2003) The structure of barley α-amylase isozyme 1 reveals a novel role of domain C in substrate recognition and binding: A pair of sugar tongs. *Structure* **11**, 973–984

6. Asatsuma, S., Sawada, C., Itoh, K., Okito, M., Kitajima, A., and Mitsui, T. (2005) Involvement of α-amylase I-1 in starch degradation in rice chloroplasts. *Plant & Cell Physiology* **46**, 858–869

7. Ziegler, P. (1988) Partial purification and characterization of the major endoamylase of mature pea leaves. *Plant Physiology* **86**, 659–666

8. Okita, T. W., Greenberg, E., Kuhn, D. N., and Preiss, J. (1979) Subcellular localization of the starch degradative and biosynthetic enzymes of spinach leaves. *Plant Physiology* **64**, 187–192

9. Kitajima, A., Asatsuma, S., Okada, H., Hamada, Y., Kaneko, K., Nanjo, Y., Kawagoe, Y., Toyooka, K., Matsuoka, K., Takeuchi, M., Nakano, A., and Mitsui, T. (2009) The rice α-amylase glycoprotein is targeted from the golgi apparatus through the secretory pathway to the plastids. *Plant Cell* **21**, 2844–2858

10. Yu, T.-S., Zeeman, S. C., Thorneycroft, D., Fulton, D. C., Dunstan, H., Lue, W.-L., Hegemann, B., Tung, S.-Y., Umemoto, T., Chapple, A., Tsai, D.-L., Wang, S.-M., Smith, A. M., Chen, J., and Smith, S. M. (2005) α-Amylase is not required for breakdown of transitory starch in Arabidopsis leaves. *Journal of Biological Chemistry* **280**, 9773–9779

11. Glaring, M. A., Baumann, M. J., Abou Hachem, M., Nakai, H., Nakai, N., Santelia, D., Sigurskjold, B. W., Zeeman, S. C., Blennow, A., and Svensson, B. (2011) Starch-binding domains in the CBM45 family; low-affinity domains from glucan, water dikinase and α-amylase involved in plastidial starch metabolism. *FEBS Journal* **278**, 1175–1185

12. Cantarel, B. L., Coutinho, P. M., Rancurel, C., Bernard, T., Lombard, V., and Henrissat, B. (2009) The Carbohydrate-Active EnZymes database (CAZy): an expert resource for glycogenomics. *Nucleic Acids Research* **37**, D233–D238

13. Mikkelsen, R., Suszkiewicz, K., and Blennow, A. (2006) A novel type carbohydrate-binding module identified in α-glucan, water dikinases is specific for regulated plastidial starch metabolism. *Biochemistry* **45**, 4674–4682

14. Zeeman, S. C., Kossmann, J., and Smith, A. M. (2010) Starch: its metabolism, evolution, and biotechnological modification in plants. *Annual Review of Plant Biology* **61**, 209–234

15. Streb, S., Delatte, T., Umhang, M., Eicke, S., Schorderet, M., Reinhardt, D., and Zeeman, S. C. (2008) Starch granule biosynthesis in Arabidopsis is abolished by removal of all debranching enzymes but restored by the subsequent removal of an endoamylase. *Plant Cell* **20**, 3448–3466

16. Streb, S., Eicke, S., and Zeeman, S. C. (2012) The simultaneous abolition of three starch hydrolases blocks transient starch breakdown in Arabidopsis. *Journal of Biological Chemistry* **287**, 41745–41756

17. Delatte, T., Umhang, M., Trevisan, M., Eicke, S., Thorneycroft, D., Smith, S. M., and Zeeman, S. C. (2006) Evidence for distinct mechanisms of starch granule breakdown in plants. *Journal of Biological Chemistry* **281**, 12050–12059

18. Kötting, O., Pusch, K., Tiessen, A., Geigenberger, P., Steup, M., and Ritte, G. (2005) Identification of a novel enzyme required for starch metabolism in Arabidopsis leaves. The phosphoglucan, water dikinase. *Plant Physiology* **137**, 242–252

19. Santelia, D., Kotting, O., Seung, D., Schubert, M., Thalmann, M., Bischof, S., Meekins, D. A., Lutz, A., Patron, N., Gentry, M. S., Allain, F. H.-T., and Zeeman, S. C. (2011) The phosphoglucan phosphatase Like Sex Four2 dephosphorylates starch at the C3-position in Arabidopsis. *Plant Cell* **23**, 4096–4111

20. McCleary, B. V., and Sheehan, H. (1987) Measurement of cereal α-amylase: A new assay procedure. *Journal of Cereal Science* **6**, 237–251

21. Anthon, G. E., and Barrett, D. M. (2002) Determination of reducing sugars with 3-methyl-2-benzothiazolinonehydrazone. *Analytical Biochemistry* **305**, 287–289

22. Smith, A. M., and Zeeman, S. C. (2006) Quantification of starch in plant tissues. *Nature Protocols* **1**, 1342–1345

23. Ficarra, R., Cutroneo, P., Aturki, Z., Tommasini, S., Calabrṇ, M., Phan-Tan-Luu, R., Fanali, S., and Ficarra, P. (2002) An experimental design methodology applied to the enantioseparation of a non-steroidal anti-inflammatory drug candidate. *Journal of Pharmaceutical and Biomedical Analysis* **29**, 989–997

24. Goodstein, D. M., Shu, S., Howson, R., Neupane, R., Hayes, R. D., Fazo, J., Mitros, T., Dirks, W., Hellsten, U., Putnam, N., and Rokhsar, D. S. (2012) Phytozome: a comparative platform for green plant genomics. *Nucleic Acids Research* **40**, D1178–1186

25. Thompson, J. D., Higgins, D. G., and Gibson, T. J. (1994) CLUSTAL W: improving the sensitivity of progressive multiple sequence alignment through sequence weighting, position-specific gap penalties and weight matrix choice. *Nucleic Acids Research* **22**, 4673–4680

26. Bak-Jensen, K. S., André, G., Gottschalk, T. E., Paës, G., Tran, V., and Svensson, B. (2004) Tyrosine 105 and threonine 212 at outermost substrate binding subsites -6 and +4 control substrate specificity, oligosaccharide cleavage patterns, and multiple binding modes of barley α-amylase 1. *Journal of Biological Chemistry* **279**, 10093–10102

27. Søgaard, M., Kadziola, A., Haser, R., and Svensson, B. (1993) Site-directed mutagenesis of histidine 93, aspartic acid 180, glutamic acid 205, histidine 290, and aspartic acid 291 at the active site and tryptophan 279 at the raw starch binding site in barley alpha-amylase 1. *Journal of Biological Chemistry* **268**, 22480–22484

28. Nielsen, J. W., Kramhøft, B., Bozonnet, S., Abou Hachem, M., Stipp, S. L. S., Svensson, B., and Willemoës, M. (2012) Degradation of the starch components amylopectin and amylose by barley α-amylase 1: Role of surface binding site 2. *Archives of Biochemistry and Biophysics* **528**, 1–6

29. Heldt, H., Werdan, K., Milovancev, M., and Geller, G. (1973) Alkalization of the chloroplast stroma caused by light-dependent proton flux into the thylakoid space. *Biochimica et Biophysica Acta* **314**, 224–241

30. Hendriks, J. H. M., Kolbe, A., Gibon, Y., Stitt, M., and Geigenberger, P. (2003) ADP-glucose pyrophosphorylase is activated by posttranslational redox-modification in response to light and to sugars in leaves of Arabidopsis and other plant species. *Plant Physiology* **133**, 838–849

31. Mikkelsen, R., Mutenda, K., Mant, A., Schürmann, P., and Blennow, A. (2005) α-Glucan, water dikinase (GWD): A plastidic enzyme with redox-regulated and coordinated catalytic activity and binding affinity. *Proceedings of the National Academy of Sciences of the United States of America* **102**, 1785–1790

32. Sparla, F., Costa, A., Lo Schiavo, F., Pupillo, P., and Trost, P. (2006) Redox regulation of a novel plastid-targeted beta-amylase of Arabidopsis. *Plant Physiology* **141**, 840–850

33. Sokolov, L. N., Dominguez-Solis, J. R., Allary, A.-L., Buchanan, B. B., and Luan, S. (2006) A redox-regulated chloroplast protein phosphatase binds to starch diurnally and functions in its accumulation. *Proceedings of the National Academy of Sciences of the United States of America* **103**, 9732–9737

34. Silver, D. M., Silva, L. P., Issakidis-Bourguet, E., Glaring, M. A., Schriemer, D. C., and Moorhead, G. B. G. (2013) Insight into the redox regulation of the phosphoglucan phosphatase SEX4 involved in starch degradation. *FEBS Journal* **280**, 538–548

35. Glaring, M. A., Skryhan, K., Kötting, O., Zeeman, S. C., and Blennow, A. (2012) Comprehensive survey of redox sensitive starch metabolising enzymes in *Arabidopsis thaliana*. *Plant Physiology and Biochemistry* **58**, 89–97

36. Meyer, Y., Buchanan, B. B., Vignols, F., and Reichheld, J.-P. (2009) Thioredoxins and glutaredoxins: unifying elements in redox biology. *Annual Review of Genetics* **43**, 335–367

37. Collin, V., Issakidis-Bourguet, E., Marchand, C., Hirasawa, M., Lancelin, J.-M., Knaff, D. B., and Miginiac-Maslow, M. (2003) The Arabidopsis plastidial thioredoxins: new functions and new insights into specificity. *Journal of Biological Chemistry* **278**, 23747–23752

38. Collin, V., Lamkemeyer, P., Miginiac-Maslow, M., Hirasawa, M., Knaff, D. B., Dietz, K.-J., and Issakidis-Bourguet, E. (2004) Characterization of plastidial thioredoxins from Arabidopsis belonging to the new *y*-type. *Plant Physiology* **136**, 4088–4095

39. Kuriki, T., and Imanaka, T. (1999) The concept of the α-amylase family: Structural similarity and common catalytic mechanism. *Journal of Bioscience and Bioengineering* **87**, 557–565

40. Williams, J. F., and Peterson, M. L. (1973) Relations between alpha-amylase activity at and growth of rice seedlings. *Crop Science* **13**, 612–615

41. Ziegler, P. (1999) Cereal beta-Amylases. *Journal of Cereal Science* **29**, 195–204

42. Scialdone, A., Mugford, S. T., Feike, D., Skeffington, A., Borrill, P., Graf, A., Smith, A. M., and Howard, M. (2013) Arabidopsis plants perform arithmetic division to prevent starvation at night. *eLife* **2**, e00669

43. Stitt, M., and Zeeman, S. C. (2012) Starch turnover: pathways, regulation and role in growth. *Current Opinion in Plant Biology* **15**, 282–292

44. Fulton, D. C., Stettler, M., Mettler, T., Vaughan, C. K., Li, J., Francisco, P., Gil, M., Reinhold, H., Eicke, S., Messerli, G., Dorken, G., Halliday, K., Smith, A. M., Smith, S. M., and Zeeman, S. C. (2008) Beta-AMYLASE4, a noncatalytic protein required for starch breakdown, acts upstream of three active beta-amylases in Arabidopsis chloroplasts. *Plant Cell* **20**, 1040–1058

45. Brandes, H. K., Larimer, F. W., and Hartman, F. C. (1996) The molecular pathway for the regulation of phosphoribulokinase by thioredoxin f. *Journal of Biological Chemistry* **271**, 3333–3335

46. Mori, H., Bak-Jensen, K. S., Gottschalk, T. E., Motawia, M. S., Damager, I., Moller, B. L., and Svensson, B. (2001) Modulation of activity and substrate binding modes by mutation of single and double subsites +1/+2 and -5/-6 of barley alpha-amylase 1. *European Journal of Biochemistry* **268**, 6545–6558

47. Zeeman, S. C., Smith, S. M., and Smith, A. M. (2007) The diurnal metabolism of leaf starch. *Biochemical Journal* **401**, 13–28

48. Wong, J. H., Kim, Y.-B., Ren, P.-H., Cai, N., Cho, M.-J., Hedden, P., Lemaux, P. G., and Buchanan, B. B. (2002) Transgenic barley grain overexpressing thioredoxin shows evidence that the starchy endosperm communicates with the embryo and the aleurone. *Proceedings of the National Academy of Sciences of the United States of America* **99**, 16325–16330

49. Buchanan, B. B., and Balmer, Y. (2005) Redox regulation: a broadening horizon. *Annual Review of Plant Biology* **56**, 187–220

50. Lemaire, S. D., Michelet, L., Zaffagnini, M., Massot, V., and Issakidis-Bourguet, E. (2007) Thioredoxins in chloroplasts. *Current genetics* **51**, 343–365

51. Schürmann, P., and Buchanan, B. B. (2008) The ferredoxin/thioredoxin system of oxygenic photosynthesis. *Antioxidants & Redox Signaling* **10**, 1235–1274

52. Hirasawa, M., Schürmann, P., Jacquot, J. P., Manieri, W., Jacquot, P., Keryer, E., Hartman, F. C., and Knaff, D. B. (1999) Oxidation-reduction properties of chloroplast thioredoxins, ferredoxin:thioredoxin reductase, and thioredoxin *f*-regulated enzymes. *Biochemistry* **38**, 5200–5205

53. Serrato, A. J., Pérez-Ruiz, J. M., Spínola, M. C., and Cejudo, F. J. (2004) A novel NADPH thioredoxin reductase, localized in the chloroplast, which deficiency causes hypersensitivity to abiotic stress in Arabidopsis thaliana. *Journal of Biological Chemistry* **279**, 43821–43827

54. Valerio, C., Costa, A., Marri, L., Issakidis-Bourguet, E., Pupillo, P., Trost, P., and Sparla, F. (2011) Thioredoxin-regulated beta-amylase (BAM1) triggers diurnal starch degradation in guard cells, and in mesophyll cells under osmotic stress. *Journal of Experimental Botany* **62**, 545–555

55. Kaplan, F., Sung, D. Y., and Guy, C. L. (2006) Roles of ß-amylase and starch breakdown during temperatures stress. *Physiologia Plantarum* **126**, 120–128

56. Weise, S., Schrader, S., Kleinbeck, K., and Sharkey, T. (2006) Carbon balance and circadian regulation of hydrolytic and phosphorolytic breakdown of transitory starch. *Plant Physiology* **141**, 879–886

57. Kaplan, F., and Guy, C. L. (2005) RNA interference of Arabidopsis beta-amylase8 prevents maltose accumulation upon cold shock and increases sensitivity of PSII photochemical efficiency to freezing stress. *Plant Journal* **44**, 730–743

Acknowledgements – We gratefully acknowledge Simone Wüthrich, Yolanda Joho-Auchli, and Dr. Peter Hunziker from the Functional Genomics Center Zürich for their assistance with the design, conduct and the analysis of the MALDI-MS experiments; Dr. Sebastian Streb for critical reading of the manuscript; Dr. Sylvain Bischof and Burak Bali for assistance with preliminary experiments; and Dr. Richard Visser (Wageningen University, Netherlands) for the amylose-free potato starch granules. We also thank two anonymous reviewers for their helpful suggestions.

FOOTNOTES

* This work was supported by the Swiss-South African Joint Research Program (to D. Santelia and S. C. Zeeman; grant IZ LS Z3122916), a SNSF Marie Heim-Vögtlin grant (to D. Santelia; grant PMPDP3_139645) and a Novartis-ETH Zurich Excellence Scholarship (to D. Seung).

FIGURE LEGENDS

FIGURE 1. *The Asp^{666} residue is essential for the amylolytic activity of AtAMY3. A*, SDS-PAGE. Purified recombinant *At*AMY3 (1 μg) and *Hv*AMY1 (1 μg) were analysed by SDS-PAGE in a 10% (w/v) gel stained with Coomassie Brilliant Blue. *B* - *C*, Activity against BPNP-G7 of *At*AMY3 WT, *At*AMY3 D666N at pH 7.9 (*B*) and *Hv*AMY1 at pH 5.5 (*C*) . The purified proteins (10 μg of *At*AMY3s and 10 ng of *Hv*AMY1) were incubated for the indicated times with an excess of BPNP-G7 and α-glucosidase at 37°C. Error bars indicate mean ± SE (n=3) and are mostly smaller than the symbols. *D*, Activity of *At*AMY3 against amylopectin and β-limit dextrin. Recombinant protein (1 μg) was incubated for 30 min with 1.5 mg solubilised substrate and the amount of reducing ends released was assayed. Values represent the mean ± SE (n=4). *E*, Activity of *Hv*AMY1 against amylopectin and β-limit dextrin. Recombinant protein (10 ng) was incubated for 10 min with 1.5 mg solubilised substrate and the amount of reducing ends released was assayed. Values represent the mean ± SE (n=3). *F*, Activity of *At*AMY3 WT and D666N on native PAGE containing 7.5% acrylamide and 0.1% amylopectin or β-limit dextrin. Recombinant proteins (1 μg) were separated by native-PAGE for 3 h at 4°C. Amylolytic activities were detected by staining with iodine solution after incubation for 1 h. Distinct *At*AMY3 activities are indicated with arrows. One representative gel from five replicate gels is shown.

FIGURE 2. *AtAMY3 releases short linear and branched malto-oligosaccharides from the starch granule surface.* Representative HPAEC-PAD chromatograms of malto-oligosaccharides released from isolated Arabidopsis starch by *At*AMY3 or *Hv*AMY1. *A*, Starch (1.5 mg) was digested with *At*AMY3 (10 μg) or *Hv*AMY1 (50 ng) and the released glucans analysed. The amounts of protein used corresponded to equal amylolytic activity against starch granules. The degree of polymerisation (DP) is indicated on top of the chromatogram. *B*, Difference plots in the chain length distribution of linear products of *At*AMY3 against native starch granules between 120 min and 30 min time points. Relative areas were calculated for each peak in chromatograms generated for *A*, yielding a percentage (relative to total peak area) for each malto-oligosaccharide species. Differences in this percentage between the 120 min and 30 min time points were plotted. Values represent the mean ± SE (n=3). *C*, Same as *B*, but for *Hv*AMY1.

FIGURE 3. *AtAMY3 releases more short branched malto-oligosaccharides from starch granules pre-treated with β-amylase.* Arabidopsis starch granules were digested as described in Figure 2. *A*, Treatment of the released glucans with *Pseudomonas* isoamylase and *Klebsiella* pullulanase resulted in smaller, linear malto-oligosaccharides, showing that the glucans were branched. Treatment with β-amylase resulted in the accumulation of maltose, maltotriose and branched glucans. The order of enzymatic treatments is indicated with arrows. *B*, Products released by *At*AMY3 from starch pre-treated with β-amylase. The order of treatments is indicated with arrows.

FIGURE 4. *AtAMY3 and AtBAM1 degrade starch synergistically in vitro.* Recombinant proteins *At*AMY3 (10 μg) and/or *At*BAM1 (2.5 μg) were incubated at 25°C with purified Arabidopsis starch

(1.5 mg). After the indicated time points, soluble glucans in the supernatant were removed and subjected to acid hydrolysis. Glucose was subsequently quantified. Values represent the mean ± SE (n=3). Error bars not visible are smaller than the symbols.

FIGURE 5. *Effect of pH on AtAMY3 and HvAMY1 activity.* The enzyme activity of *At*AMY3 (*A*, 10 μg) and *Hv*AMY1 (*B*, 10 ng) was assayed in Britton-Robinson buffer under the standard assay conditions, where pH of the mixture was titrated as indicated (pH 5-8.5). The reactions were stopped after 60 min for *At*AMY3, and 20 min for *Hv*AMY1. Values represent the mean ± SE (n=3). Error bars not visible are smaller than the symbols. Note the difference in the y-axis scale between *A* and *B*.

FIGURE 6. *Redox regulation of AtAMY3 activity. A - B*, Redox sensitivity of *At*AMY3 and *Hv*AMY1. Purified recombinant proteins were exposed to 5 mM DTT or 50 μM $CuCl_2$ for 2 h prior to activity assay. Reduced and oxidised proteins were then incubated for 2 h with or without 20 mM DTT prior to assaying activity. Values represent the mean ± SE (n=4). Note the difference in the y-axis scale between *A* and *B*. *C*, In-gel reactivation of oxidised *At*AMY3 protein. Recombinant *At*AMY3 was run on a native polyacrylamide gels containing amylopectin. Lanes were incubated with 5 mM DTT (1) or 25 μM $CuCl_2$ (2) for 1 h prior to staining in Lugol solution. Lanes incubated with 25 μM $CuCl_2$ were rinsed in washing buffer and further incubated with (4) or without (3) 20 mM DTT for a further 3 h prior to staining in Lugol solution. *D*, In-gel redox regulation of native *At*AMY3 enzyme. Arabidopsis leaf crude extracts from 4-week-old Col-0 wild type and *amy3* mutant plants were separated on native polyacrylamide gels containing amylopectin. Lanes were incubated with 5 mM DTT (1) or 100 μM $CuCl_2$ (2) for 3 h prior to staining in Lugol solution. Lanes incubated with 100 μM $CuCl_2$ were rinsed in washing buffer and further incubated overnight with (4) or without (3) 20 mM DTT prior to staining in Lugol solution. To exclude the possibility that other *At*AMY3 bands with undetectable activity may be present, an immunoblot was probed with an anti-*At*AMY3 antibody (5).

FIGURE 7. *Midpoint redox potential of AtAMY3 at pH 7.9.* The ambient redox potential (E_h), adjusted by defined ratios of $DTT_{oxidised}/DTT_{reduced}$, ranged from -270 to -420 mV. Pre-oxidised *At*AMY3 protein (10 μg) was incubated in tricine-NaOH buffer containing 20 mM total DTT in different dithiol/disulfide ratios for 2 h prior to assaying activity. The midpoint redox potential at this pH ($E_{m,\,7.9}$) was calculated by fitting the Nernst equation, and the error is the SEM calculated from three replicate experiments.

FIGURE 8. *C587S site-specific mutant of AtAMY3 is redox insensitive.* Purified *At*AMY3 and its cysteine mutant variants (1 μg each) were electrophoresed on native polyacrylamide gels containing amylopectin. Gels were incubated with 5 mM DTT (A) or 50 μM $CuCl_2$ (B) for 3 h prior to staining in Lugol solution. Gels incubated with 50 μM $CuCl_2$ were rinsed in washing medium and further incubated overnight with (D) or without (C) 20 mM DTT prior to staining in Lugol solution.

FIGURE 9. *A disulfide linkage between Cys^{499} and Cys^{587} identified using mass spectrometry.* Reduced and oxidised proteins were digested in solution with LysC, and the resulting peptides were analysed by MALDI-MS/MS. *A-B*, Mass spectra of two peptides generated from the digest of reduced and oxidised wild type proteins. The peptides at 1679.9 m/z (A) and 2361.1 m/z (B) correspond to Cys^{587} and Cys^{499} containing peptides respectively (Table 4). (C) Mass spectra generated from digested reduced and oxidised wild type proteins, as well as oxidised C499S and C587S variants. A disulfide-linked peptide at the additive mass of peptides shown in *A* and *B* can be observed at 4038.0 m/z, exclusively in the oxidised wild-type protein.

Table 1

TABLE 1
Quantification of peak areas from Figure 2A. Values represent relative peak areas from HPAEC-PAD chromatograms of malto-oligosaccharides released from Arabidopsis starch granules by *At*AMY3 or *Hv*AMY1. Starch (1.5 mg) was digested with *At*AMY3 (10 μg) or *Hv*AMY1 (50 ng) for 30 min or 120 min, and the glucans released were analysed. A representative chromatogram is presented in Figure 2A. The relative peak area was calculated for each peak as a percentage of total peak area. Values represent the mean ± SE from chromatograms produced from three replicate digests.

		*At*AMY3		*Hv*AMY1	
	DP	30 min	120 min	30 min	120 min
Linear glucans	3	4.00 ± 0.09	5.71 ± 0.03	2.78 ± 0.05	4.28 ± 0.03
	4	9.8 ± 0.1	12.28 ± 0.04	2.878 ± 0.008	3.78 ± 0.03
	5	7.00 ± 0.03	7.96 ± 0.01	1.191 ± 0.006	1.87 ± 0.02
	6	13.60 ± 0.06	16.07 ± 0.05	10.38 ± 0.02	13.0 ± 0.1
	7	22.76 ± 0.05	23.68 ± 0.01	34.1 ± 0.2	36.6 ± 0.3
	8	16.74 ± 0.05	13.70 ± 0.05	15.5 ± 0.2	13.66 ± 0.03
	9	10.19 ± 0.07	5.49 ± 0.06	7.96 ± 0.08	6.06 ± 0.01
	10	4.47 ± 0.07	1.09 ± 0.03	6.13 ± 0.06	4.33 ± 0.02
	11	1.03 ± 0.03	0.162 ± 0.008	4.42 ± 0.05	2.96 ± 0.01
	12	0.293 ± 0.007	0.096 ± 0.004	3.42 ± 0.04	2.22 ± 0.01
	13	0.186 ± 0.003	0.133 ± 0.001	2.60 ± 0.03	1.669 ± 0.007
	14	0.137 ± 0.002	0.162 ± 0.002	1.92 ± 0.03	1.245 ± 0.007
	15	0.119 ± 0.002	0.248 ± 0.002	1.31 ± 0.02	0.824 ± 0.002
Branched glucans	8	0.08 ± 0.04	0.295 ± 0.002	0.009 ± 0.009	0.07 ± 0.04
	9	0.31 ± 0.02	0.82 ± 0.01	0.303 ± 0.003	0.546 ± 0.006
	10	0.838 ± 0.007	1.64 ± 0.01	0.639 ± 0.004	0.942 ± 0.007
	11	1.30 ± 0.01	2.19 ± 0.02	0.537 ± 0.004	0.881 ± 0.007
	12	1.539 ± 0.004	2.17 ± 0.01	0.550 ± 0.005	0.91 ± 0.01
	13	1.596 ± 0.004	1.965 ± 0.007	0.622 ± 0.003	0.96 ± 0.01
	14	1.534 ± 0.005	1.66 ± 0.001	0.635 ± 0.005	0.941 ± 0.009
	15	1.345 ± 0.008	1.275 ± 0.002	0.545 ± 0.002	0.763 ± 0.004

Table 2

TABLE 2.
Reactivation of oxidised *At*AMY3 protein by different isoforms of Arabidopsis chloroplastic thioredoxins (*At*Trx). 10 μg of recombinant *At*AMY3 was initially oxidised by 50 μM $CuCl_2$ and then incubated with various *At*Trx isoforms (5 μM) in the presence of 0.05 mM DTT for 30 min before assaying the activity. Trx *f*, *m*, *x* and *y* isoforms from Arabidopsis were purified recombinant proteins expressed in *E. coli*. Values represent the mean ± SE (n=3).

	DTT (mM)	Thioredoxin (5 μM)	PNP released (nmol min^{-1} mg^{-1})	% of reduced activity
Reduced protein	0	-	26.2 ± 0.3	
	20	-	26.3 ± 0.7	100
Oxidised protein	0	-	1.22 ± 0.05	5
	0.05	-	3.8 ± 0.3*	14
		Trx *f1*	15.4 ± 0.3*	59
		Trx *m1*	12.3 ± 0.4*	47
		Trx *m2*	11.8 ± 0.5*	45
		Trx *m3*	6.6 ± 0.3*	25
		Trx *m4*	9.4 ± 0.4*	36
		Trx *x*	9.0 ± 0.4*	34
		Trx *y1*	11.1 ± 0.6*	42
		Trx *y2*	13.6 ± 0.8*	52
		E. coli Trx	13.9 ± 0.3*	53

* denotes significant difference from oxidised protein without DTT or Trx with a two-tailed t-test ($P < 0.05$)

Table 3

TABLE 3.
Activity of *At*AMY3 and its cysteine mutant variants against BPNP-G7 under reducing or oxidising conditions. Purified recombinant proteins (10 μg) were exposed to 5 mM DTT or 50 μM $CuCl_2$ for 1 h prior to activity assay. Values represent the mean ± SE (n=3)

	Reduced activity	Oxidised activity	
	nmol min^{-1} mg^{-1}	nmol min^{-1} mg^{-1}	% of reduced activity
WT	31.6 ± 0.5	0.06 ± 0.03	< 1% *
C118S	27.7 ± 0.5	0.06 ± 0.03	< 1% *
C285S	11.1 ± 0.6	0.14 ± 0.05	1% *
C310S	21.7 ± 0.4	0.03 ± 0.03	< 1% *
C363S	44.4 ± 0.4	0.13 ± 0.03	< 1% *
C499S	2.4 ± 0.1	0 ± 0	0% *
C587S	3.9 ± 0.2	3.3 ± 0.2	85%
C652S	17.2 ± 0.3	0.06 ± 0.03	< 1% *
C743S	29.1 ± 0.5	0.6 ± 0.3	2% *
C832S	33.3 ± 0.7	0 ± 0	0% *

* denotes significant difference ($P < 0.05$) between reduced and oxidised activities with a two-tailed t-test

Table 4

TABLE 4.
*At*AMY3 peptides confirmed by MALDI-MS/MS. Peptides generated after in-solution digest with LysC were visualised by MALDI-MS (Fig. 8), and the corresponding MS/MS spectra were searched with Mascot against the recombinant protein sequence. Mascot scores are from spectra generated with the reduced wild type protein.

m/z	Peptide		Score
1679.9	VLGDAVLNHRC*AHFK	*Cys_{587}	70
2361.1	ISSGTGSGFEILC*QGFNWESNK	*Cys_{499}	91

Figure 1

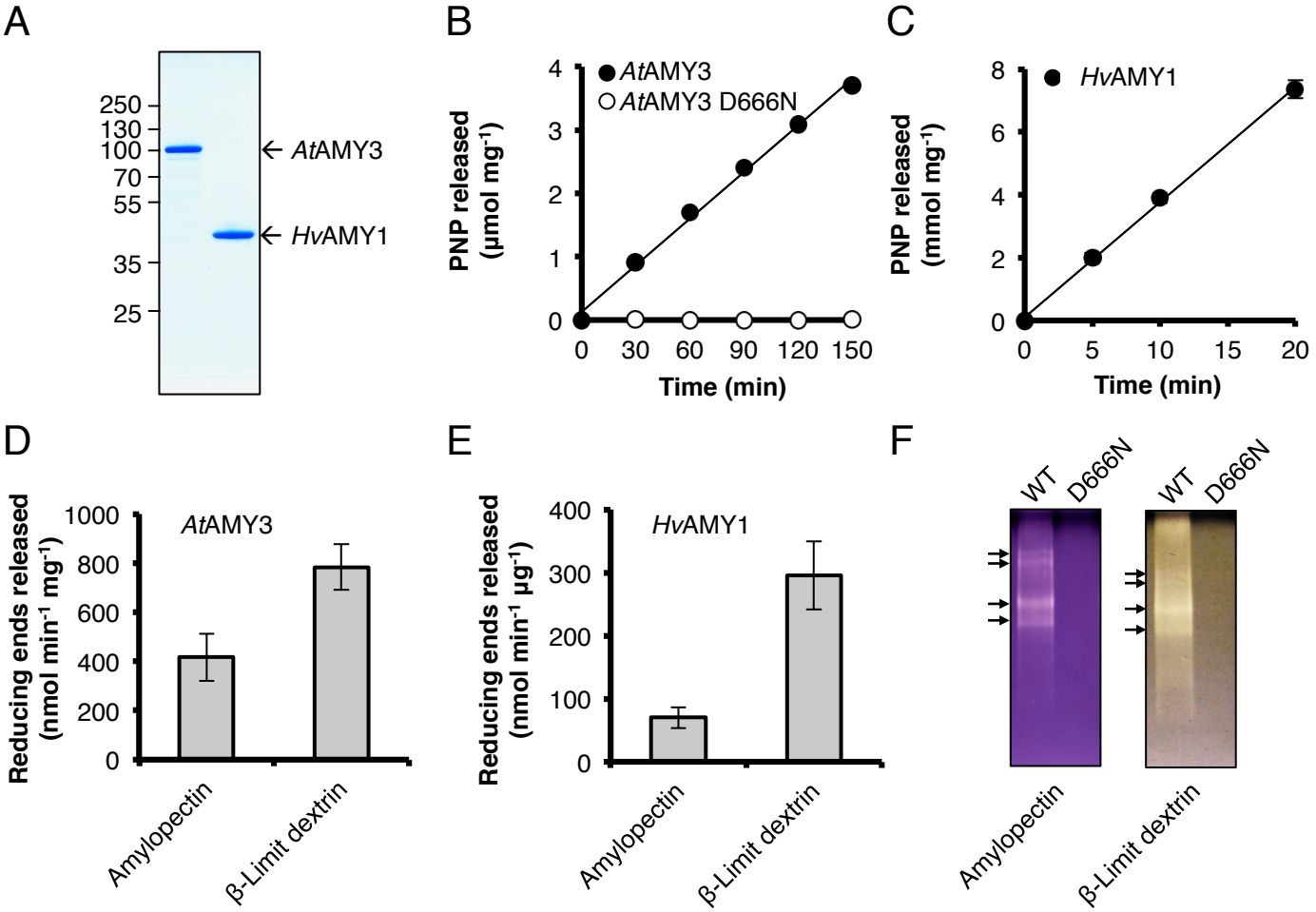
A
250
130
100
70
55
35
25
← AtAMY3
← HvAMY1
B
AtAMY3
AtAMY3 D666N
PNP released (µmol mg-1)
Time (min)
C
HvAMY1
PNP released (mmol mg-1)
Time (min)
D
AtAMY3
Reducing ends released (nmol min-1 mg-1)
Amylopectin
β-Limit dextrin
E
HvAMY1
Reducing ends released (nmol min-1 µg-1)
Amylopectin
β-Limit dextrin
F
WT
D666N
WT
D666N
Amylopectin
β-Limit dextrin

Figure 2

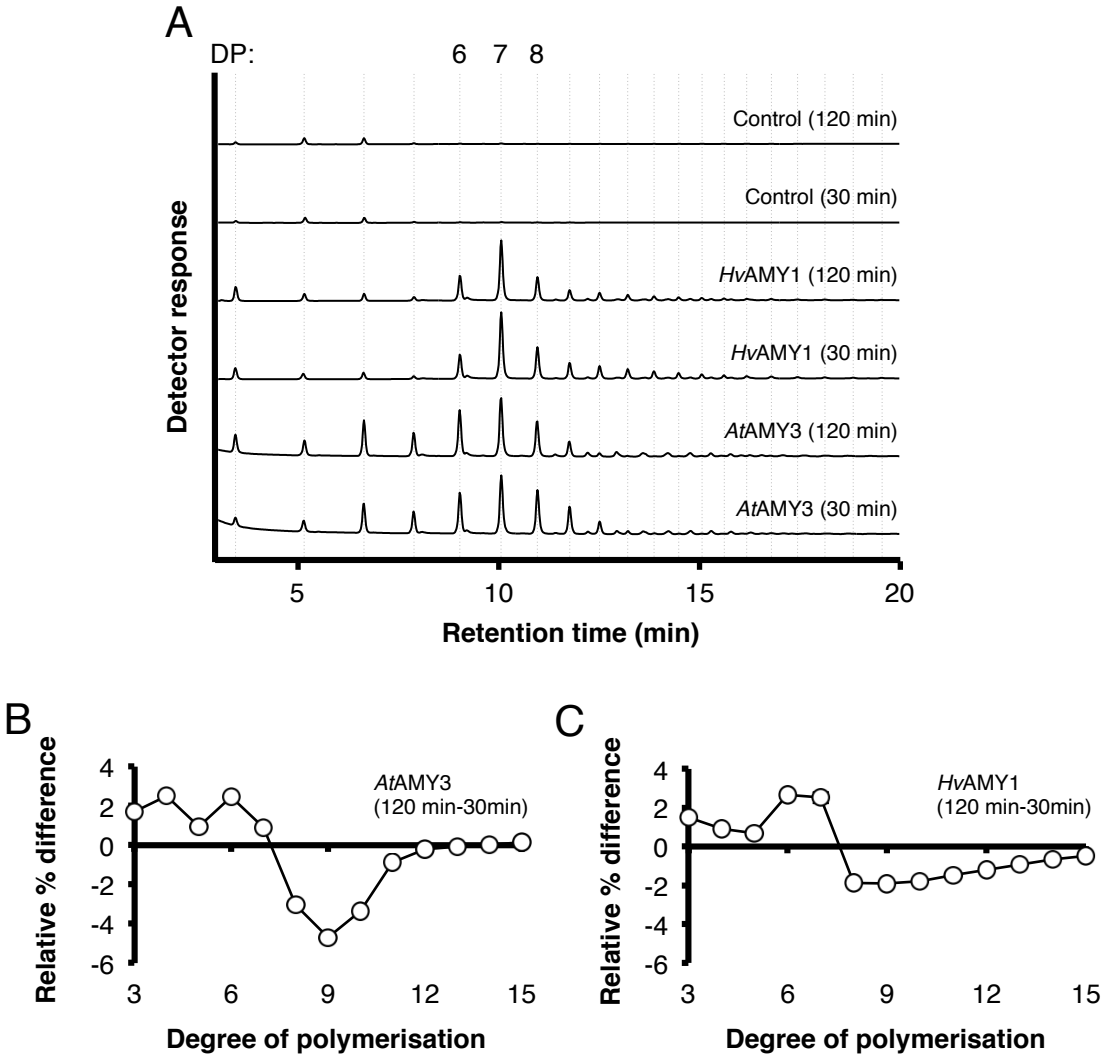
A
DP:
6 7 8
Control (120 min)
Control (30 min)
HvAMY1 (120 min)
HvAMY1 (30 min)
AtAMY3 (120 min)
AtAMY3 (30 min)
Detector response
5
10
15
20
Retention time (min)
B
Relative % difference
4
2
0
-2
-4
-6
AtAMY3
(120 min-30min)
3
6
9
12
15
Degree of polymerisation
C
Relative % difference
HvAMY1
(120 min-30min)
Degree of polymerisation

Figure 3

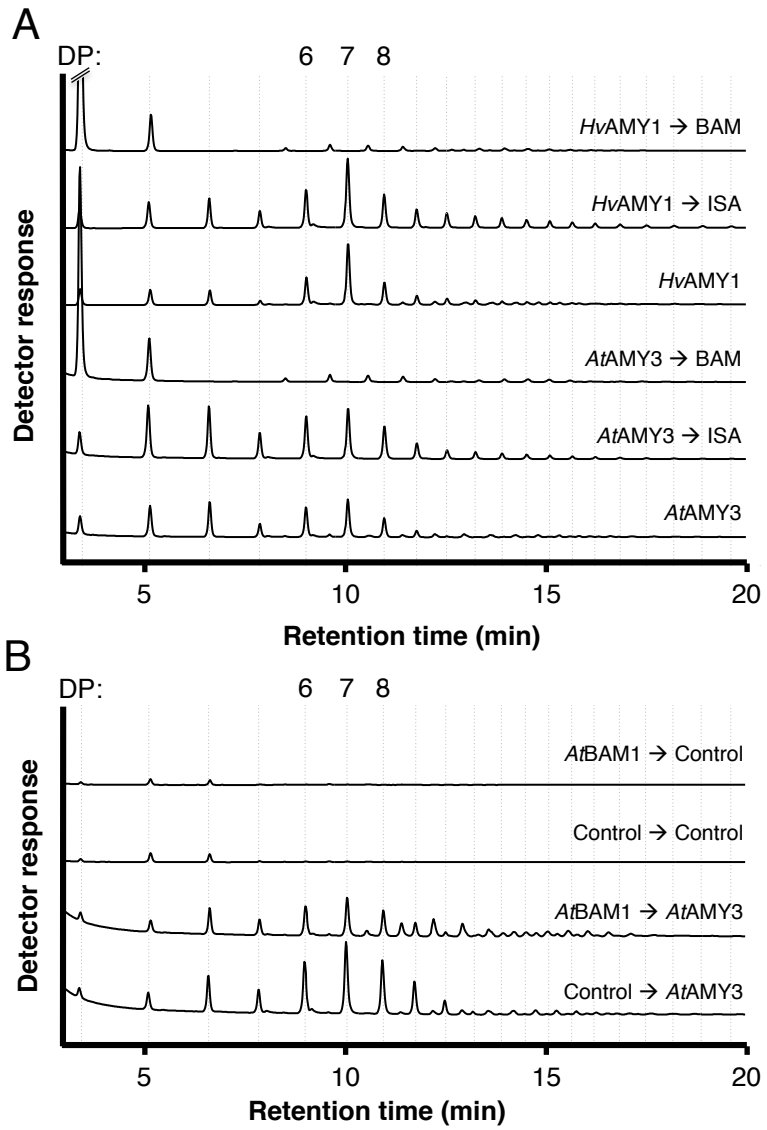
A
DP:
6 7 8
HvAMY1 → BAM
HvAMY1 → ISA
HvAMY1
AtAMY3 → BAM
AtAMY3 → ISA
AtAMY3
Detector response
5
10
15
20
Retention time (min)
B
DP:
6 7 8
AtBAM1 → Control
Control → Control
AtBAM1 → AtAMY3
Control → AtAMY3
Detector response
5
10
15
20
Retention time (min)

Figure 4

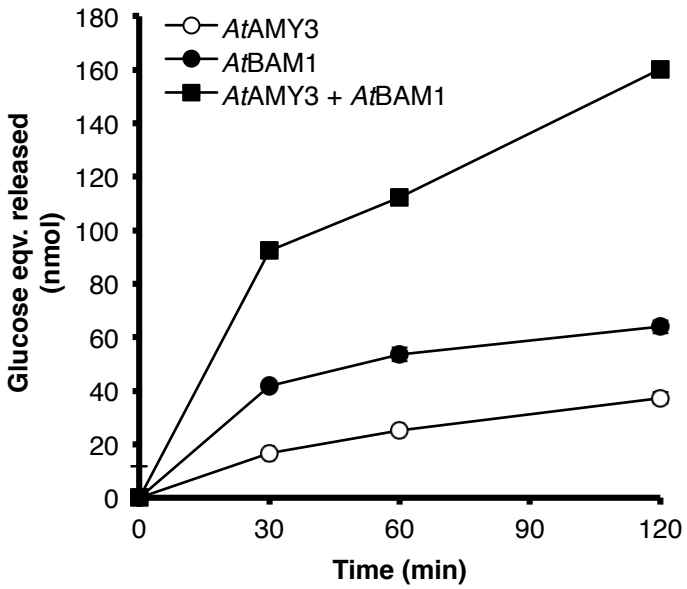
180
160
140
120
100
80
60
40
20
0
Glucose eqv. released (nmol)
*At*AMY3
*At*BAM1
*At*AMY3 + *At*BAM1
0
30
60
90
120
Time (min)

Figure 5

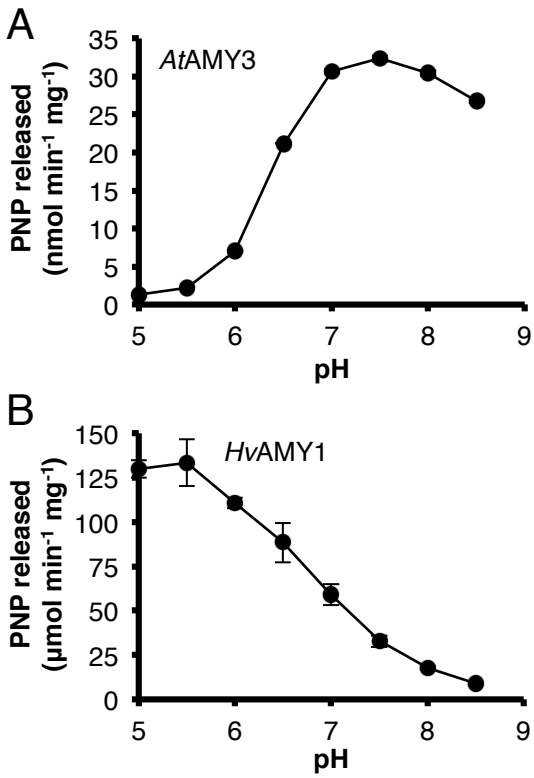
A
*At*AMY3
PNP released
(nmol min-1 mg-1)
35
30
25
20
15
10
5
0
5
6
7
8
9
pH
B
*Hv*AMY1
PNP released
(µmol min-1 mg-1)
150
125
100
75
50
25
0
5
6
7
8
9
pH

Figure 6

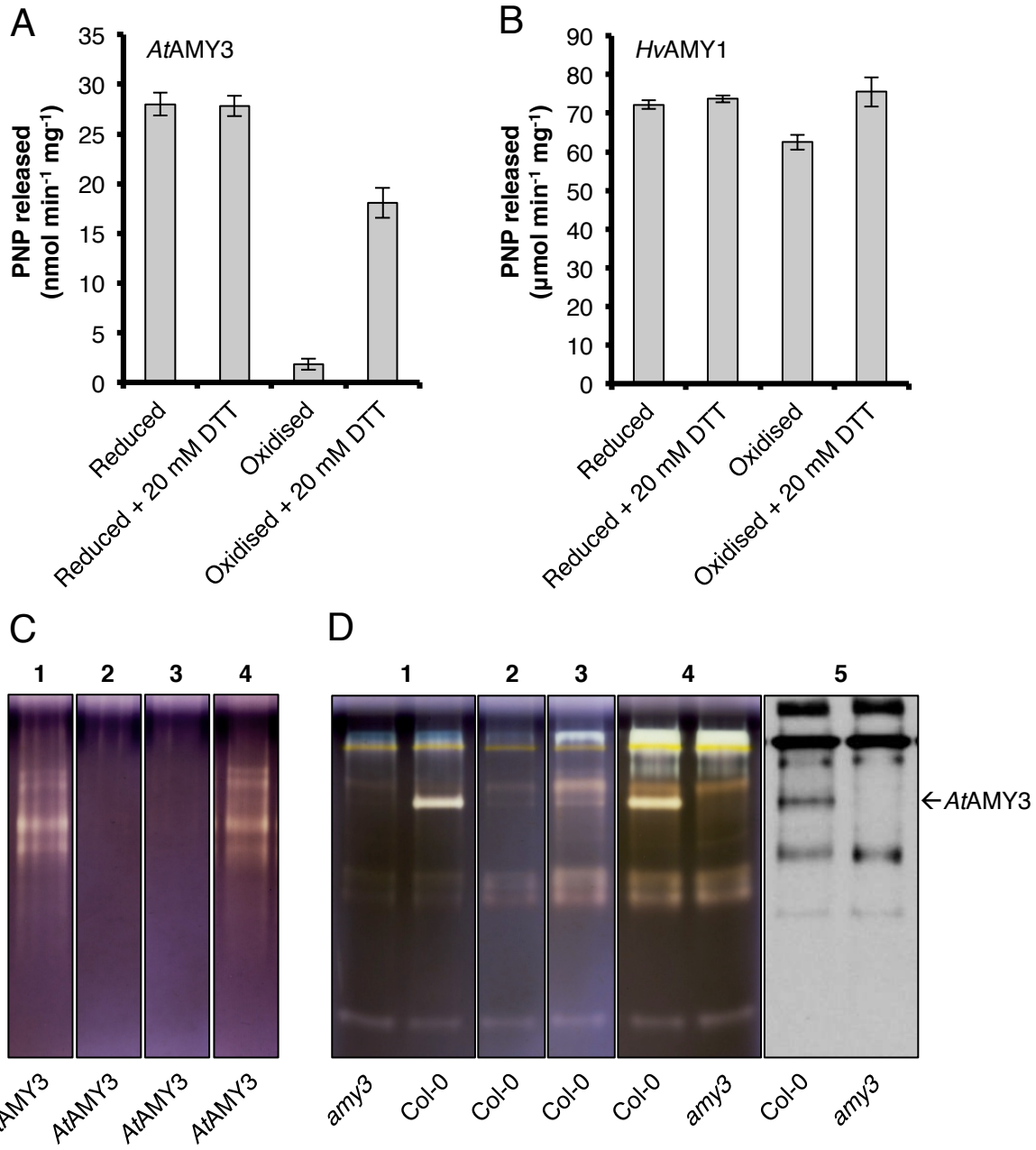
A
*At*AMY3
PNP released (nmol min-1 mg-1)
35
30
25
20
15
10
5
0
Reduced
Reduced + 20 mM DTT
Oxidised
Oxidised + 20 mM DTT
B
*Hv*AMY1
PNP released (µmol min-1 mg-1)
90
80
70
60
50
40
30
20
10
0
Reduced
Reduced + 20 mM DTT
Oxidised
Oxidised + 20 mM DTT
C
1
2
3
4
*At*AMY3
*At*AMY3
*At*AMY3
*At*AMY3
D
1
2
3
4
5
←*At*AMY3
amy3
Col-0
Col-0
Col-0
Col-0
amy3
Col-0
amy3

Figure 7

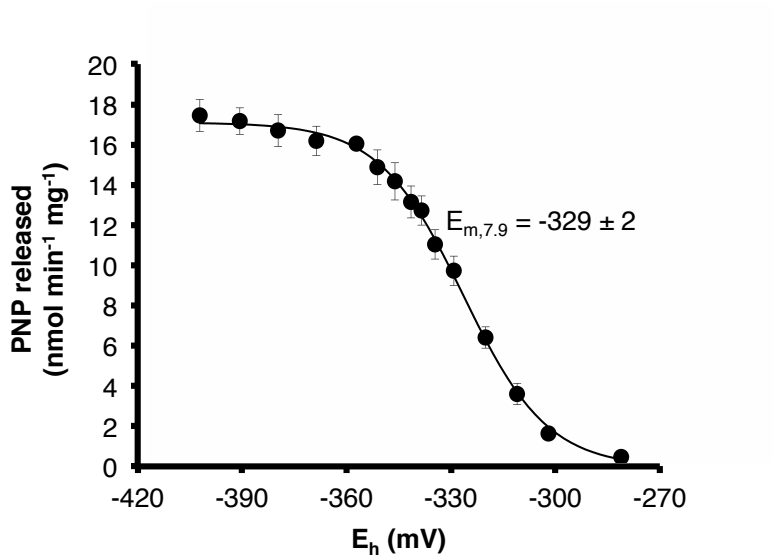
PNP released
(nmol min-1 mg-1)
20
18
16
14
12
10
8
6
4
2
0
-420
-390
-360
-330
-300
-270
Eh (mV)
Em,7.9 = -329 ± 2

Figure 8

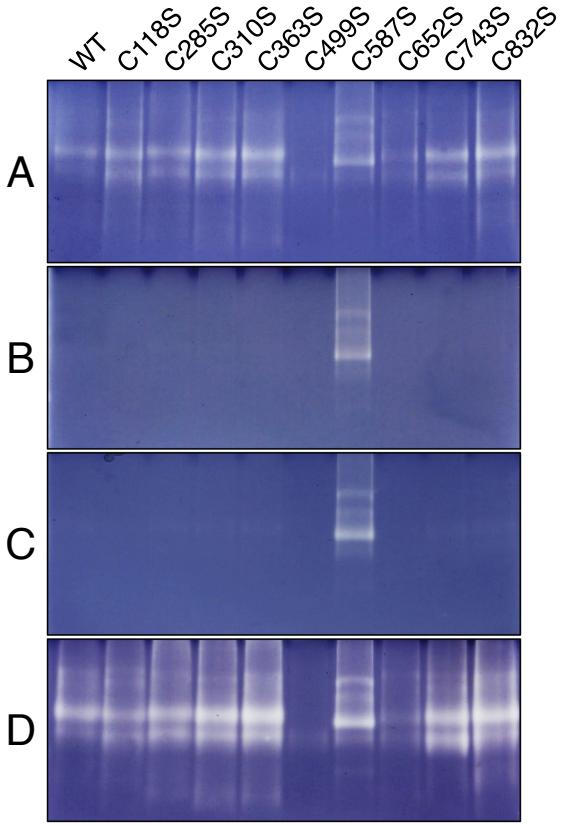
WT
C118S
C285S
C310S
C363S
C499S
C587S
C652S
C743S
C832S
A
B
C
D

Figure 9

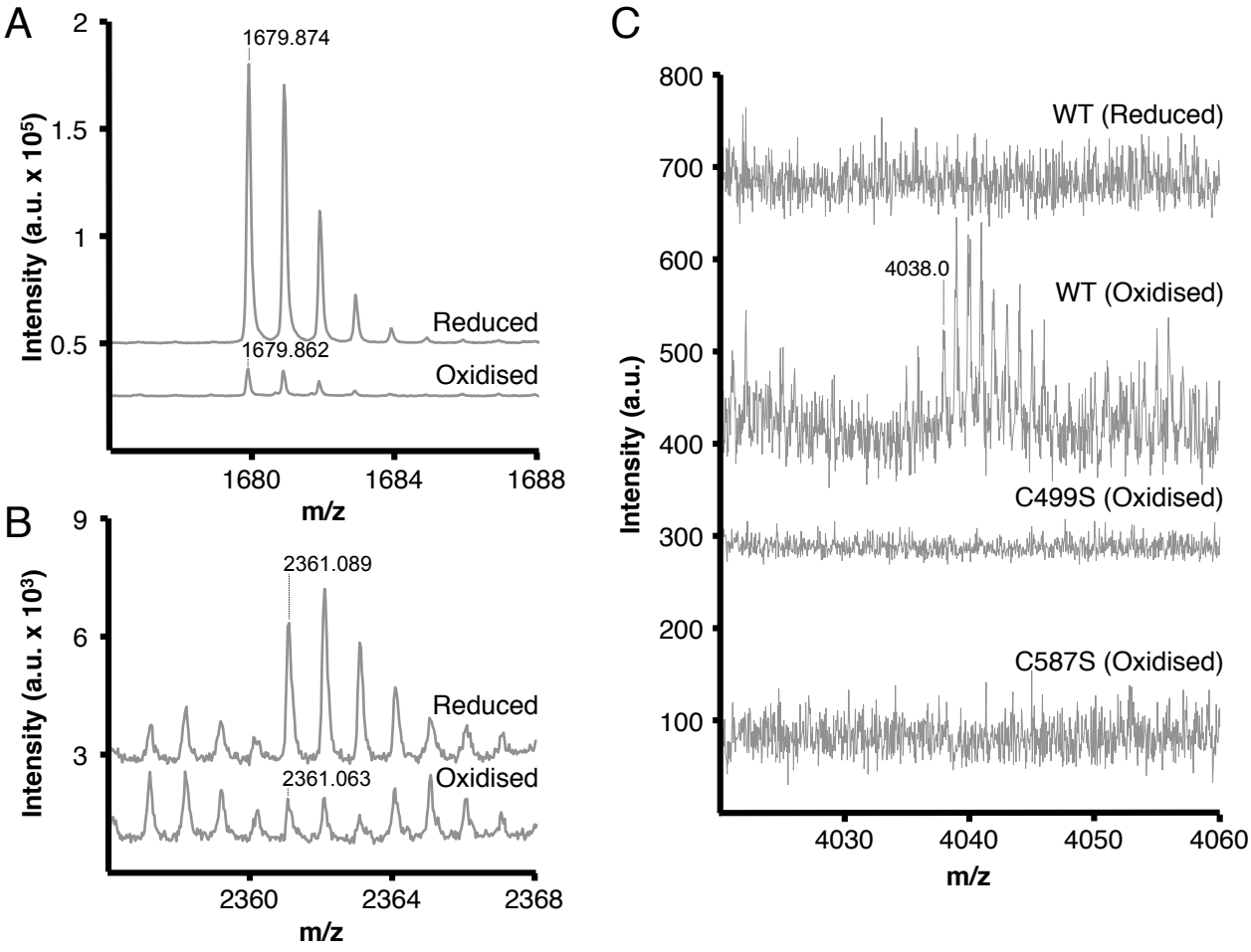
A
1679.874
1679.862
Reduced
Oxidised
Intensity (a.u. x 10⁵)
m/z
B
2361.089
2361.063
Reduced
Oxidised
Intensity (a.u. x 10³)
m/z
C
WT (Reduced)
4038.0
WT (Oxidised)
C499S (Oxidised)
C587S (Oxidised)
Intensity (a.u.)
m/z